LA-10032-PR
Progress Report

UC-70
Issued: August 1984

Research and Development Related to the Nevada Nuclear Waste Storage Investigations

October 1—December 31, 1983

Compiled by

K. Wolfsberg
D. T. Vaniman

Contributors

D. L. Bish
J. D. Blacic
N. W. Bower
D. E. Broxton
F. M. Byers, Jr.
B. A. Carlos
M. R. Cisneros
B. M. Crowe
D. Croy
D. B. Curtis
C. J. Duffy
R. R. Geoffrion
R. C. Gooley
L. E. Hersman
D. E.Hobart
J. F. Kerrisk
S. D. Knight
F. O. Lawrence
S. S. Levy
C. W. Myers
D. C. Nelson
T. W. Newton
H. Nitsche*
A. E. Norris
A. E. Ogard
D. M. Roy**
J. C. Rowley
R. S. Rundberg
V. L. Rundberg
K. W. Thomas
J. L. Thompson
B. J. Travis
D. T. Vaniman
K. Wolfsberg
D. A. York

*Materials and Molecular Research Division, Lawrence Berkeley Laboratory, Berkeley, CA 94720.
**Materials Research Laboratory, The Pennsylvania State University, University Park, PA 16802.

Los Alamos National Laboratory
Los Alamos, New Mexico 87545

CONTENTS

ABSTRACT 1

EXECUTIVE SUMMARY 2

I. INTRODUCTION 9

II. GEOCHEMISTRY 11
- A. Groundwater Chemistry 11
- B. Natural Isotope Chemistry 12
- C. Hydrothermal Geochemistry 12
- D. Solubility Determination 19
  - 1. Am··tcium Thermodynamic Data 19
  - 2. Pl··onium Chemistry in Near-Neutral Solutions 20
  - 3. Determination of Solubilities and Complexation of Waste Radionuclides Pertinent to Geologic Disposal . . . 21
  - 4. Colloids 25
- E. Sorption and Precipitation 26
  - 1. Batch Sorption Experiments of Sorption and Precipitation 26
  - 2. Long-Term Sorption Experiments on Technetium and Neptunium 26
  - 3. Cation Exchange Capacity of Tuffs 29
  - 4. Microbiological Activity at Yucca Mountain 33
- F. Dynamic Transport Process 36
- G. Retardation Sensitivity Analysis 44
  - 1. Heat Load Effects 44
  - 2. Field Study of Radionuclide Transport in Unsaturated, Fractured Tuff 53
  - 3. Colloid Formation and Migration Modeling 54
- H. Applied Diffusion 54

III. MINERALOGY-PETROLOGY OF TUFF 56
- A. New Data on Clinoptilolite Composition 56
- B. Heating Experiments on Cristobalite, Clinoptilolite, and Heulandite 59
- C. Petrologic Studies of the Topopah Spring Member and Drill Hole UE-25p#1 60

IV. TECTONICS AND VOLCANISM 63

V. TUFF LABORATORY PROPERTIES 65

VI. SEALING MATERIALS EVALUATION 66

VII. EXPLORATORY SHAFT 69
- A. Technical Direction-Design 69
- B. Test Plan 70
- C. Integrated Data System 71

VIII. QUALITY ASSURANCE 72
- A. Los Alamos 72
- B. USGS 72

REFERENCES 73

RESEARCH AND DEVELOPMENT RELATED TO THE NEVADA NUCLEAR WASTE STORAGE INVESTIGATIONS

October 1--December 31, 1983

Compiled by

K. Wolfsberg and D. T. Vaniman

Contributors

D. L. Bish
J. D. Blacic
N. W. Bower
D. E. Broxton
F. M. Byers, Jr.
B. A. Carlos
M. R. Cisneros
B. M. Crowe
D. Croy
D. B. Curtis
C. J. Duffy
R. R. Geoffrion
R. C. Gooley
L. E. Hersman
D. E. Hobart
J. F. Kerrisk
S. D. Knight
F. O. Lawrence
S. S. Levy
C. W. Myers
D. C. Nelson
T. W. Newton
H. Nitsche
A. E. Norris
A. E. Ogard
D. M. Roy
J. C. Rowley
R. S. Rundberg
V. L. Rundberg
K. W. Thomas
J. L. Thompson
B. J. Travis
D. T. Vaniman
K. Wolfsberg
D. A. York

ABSTRACT

This report summarizes the contribution of the Los Alamos National Laboratory to the Nevada Nuclear Waste Storage Investigations for the first quarter of FY 1984.

EXECUTIVE SUMMARY

This report summarizes some technical contributions by the Los Alamos National Laboratory to the Nevada Nuclear Waste Storage Investigations (NNWSI) project managed by the Nevada Operations Office of the US Department of Energy (DOE) during the period October 1 through December 31, 1983. The report is not a detailed technical document but does indicate the status of the investigations being performed at Los Alamos.

GEOCHEMISTRY

Technical progress was somewhat limited this quarter because much of the attention of the NNWSI Task Leaders was directed towards the geochemistry contribution for the NNWSI Environmental Assessment Report.

Groundwater Chemistry

The pumping test on Well USW H-3 has been started. The objectives of this test are (1) to determine the composition of formation water from a test hole in the southern part of the repository block near the Nevada Test Site (NTS), (2) to obtain formation water from a zone with low permeability, and (3) to obtain additional data for determining transmissivity of a selected interval in this well. The packer that was in place for potentiostat measurements has been removed. An external casing packer was installed at 2694 to 2697 ft below ground surface (~225 ft below the standing water level in the hole). A Moyno rotary pump was installed at ~3000 ft below the land surface with an access line running beside it. The access line will be used by the US Geological Survey (USGS) to insert a pressure transducer for determining changes in water level during pumping. The pump produced water at 2.3 gal./minute but was shut down and pulled back up for inspection because of excess drag somewhere in the system.

Natural Isotope Chemistry

A contract has been negotiated for services to determine the infiltration profile of the ^{36}Cl bomb pulse at Yucca Mountain and to interpret the data for hydrologic infiltration rates. This pulse was created when a large amount of ^{36}Cl, 3 orders of magnitude above natural background level, was injected into the stratosphere by weapon tests in the Pacific between 1952

and 1958. The injection resulted in a pulse of global fallout between 1953 and 1964. This tracer pulse has been used for hydrologic studies of recent water movement, including a study of transit and recharge rates in an arid region. An ultrasensitive technique employing a tandem-accelerator mass spectrometer must be employed in the detection of the ^{36}Cl nuclide (300 000-year half-life). Samples over a few meters depth will be taken from four locations in alluvium and fractured tuff on Yucca Mountain or in its washes. Chloride and ^{36}Cl profiles will be measured on the samples.

Hydrothermal Geochemistry

The question of clinoptilolite and mordenite stability is important in assessing the suitability of Yucca Mountain as a nuclear waste repository because the sorptive capacity of the tuff would be reduced by the possible breakdown of these minerals. It has been suggested that clinoptilolite is stable to about 100°C and mordenite is likely stable to higher temperatures. Very little of the clinoptilolite or mordenite in Yucca Mountain is likely to experience temperatures as high as 100°C, as a result of repository heating. However, there is considerable evidence that clinoptilolite and mordenite may be stabilized by a metastably high chemical potential of SiO_2, such as would be in equilibrium with cristobalite or glass, but not with quartz. Where the chemical potential of SiO_2 is controlled by equilibrium with quartz, clinoptilolite and mordenite may not be stable, even at 2[illegible].

The rate at which cristobalite may convert to quartz has been modeled with a simple dissolution precipitation model. It suggests that, where cristobalite is still present in Yucca Mountain, either a continuous fluid phase has not been present (except perhaps for short periods of time), or movement of SiO_2 in the fluid rather than across quartz/fluid and cristobalite/fluid interfaces has been the rate-controlling step in the cristobalite-to-quartz transition.

Solubility Determination

A thermodynamic data file for americium has been completed for the EQ3/6 chemical equilibirum computer program. Although there is still considerable uncertainty about the identity and formation constants of some americium species, the solubility of americium in Well J-13 water was calculated as 1.0×10^{-8} M on the basis of available data.

A paper describing measurements of rates of disproportionation and polymerization of Pu(IV) was presented at the Seventh International Symposium on the Scientific Basis for Nuclear Waste Management and is abstracted in this report.

Disproportionation of Pu(V) is being studied in an attempt to obtain thermodynamic data for the hydrous oxide of plutonium.

Experiments have been initiated to determine whether microcolloidal actinide particles may be involved in laboratory sorption measurements.

To better characterize the actinide species in laboratory sorption measurements, it is necessary to determine whether colloidal particles with diameters <50 nm may be initially present or may be forming in the feed solutions employed for sorption studies. Observations to date indicate that some filterable particles (with diameters >50 nm) may form when solutions 10^{-7} to 10^{-9} M in americium are aged for several days. However, the evidence is ambigious because sorption also increases with these aged solutions. Work is continuing with more dilute solutions.

Sorption and Precipitation

Long-term sorption experiments with neptunium and technetium show that the measured sorption ratio does not change over a period of up to 3 months. This study will be carried out to 15 months to determine if there are any changes in the ratios at even longer times.

Sorption/desorption measurements from crushed-tuff (batch) experiments were shown to be in excellent agreement with corresponding measurements on intact 2-mℓ-thick tuff wafers.

The cation exchange capacity values of tuff samples used in sorption studies were measured. Earlier work has shown that cation exchange capacity values of tuff minerals are correlated with sorption ratios with mineralogy. Using a multiple-regression least squares program, work has begun in evaluating the cation exchange capacity values against mineralogy.

The regrowth of bacteria during sorption experiments evidently compromised the experiments. However, there is some indication that the presence of bacteria enhances sorption of plutonium on tuff. More extensive studies are planned. Other preliminary bacteria experiments indicate that the presence of bacteria lead to an increase in the viscosity of the drilling polymer.

Dynamic Transport Process

The sorption of simple cations in tuff is dominated by adsorption on aluminosilicates that have charged surfaces, such as zeolites and clays. The most significant sorbing minerals present in Yucca Mountain tuffs are clinoptilolite, heulandite, mordenite, and montmorillonite. The kinetics of sorption on tuffs containing the minerals clinoptilolite and montmorillonite has been determined by studying the uptake of strontium, cesium, and barium on thin tuff wafers. The rate constants for uptake of these elements on tuff are consistent with a model of sorption in which diffusion is limited but where diffusion occurs in two stages. First, the cations diffuse into the rock through the water-filled pore space. Next, the cations must diffuse into the much narrower channels within the aluminosilicate crystals. After they are within the zeolite framework or in the interlayer volume in the clays, the cations may rapidly sorb on the negatively charged surfaces. The actinide elements have a time constant for the apparent sorption that is inconsistent with this model and may have a radically different mechanism of removal from solution.

Retardation Sensitivity Analysis

Several topics were studied during this quarter: (1) additional calculations of heat load effects from a waste repository in Yucca Mountain, (2) a field study of plutonium and americium transport in fractured, unsaturated tuff at Los Alamos, and (3) model equations for colloid transport.

Applied Diffusion

A plan for measuring diffusion rates in field experiments at Yucca Mountain has been prepared and included in NVO-244, Rev.0, "Test Plan for Exploratory Shaft at Yucca Mountain." Diffusivities will be measured for solutes that diffuse from solutions into the water-filled pore spaces both in the Yucca Mountain nuclear waste repository host rock and in the underlying tuffaceous beds of Calico Hills.

MINERALOGY-PETROLOGY OF TUFF

New data were obtained on clinoptilolite compositions from UE-25a#1, UE-26b#1, and UE-25p#1. In these drill holes, the clinoptilolites at all

depths have higher concentrations of calcium (and magnesium) than of potassium and sodium. The lack of alkali enrichment with depth is unlike the compositional zonation observed in Drill Holes USW G-1, USW G-2, and USW G-3. Further data now being collected may help constrain the possible models of exchangeable cation zonation and zeolite origins at Yucca Mountain.

Heating experiments on samples from Yucca Mountain have determined a temperature of 225 ± 25°C for the transition from α to β cristobalite, with a volume increase of 5%. Other heating experiments indicate that the temperature of inversion from heulandite to heulandite-B is higher in microcrystalline Yucca Mountain samples (>200°C) than in the more "ideal" macrocrystalline samples obtained from basalts as standard heulandite (>150°C). Work is in progress to determine the kinetics of this inversion, which may affect the sorptive zeolites closest to the repository.

TECTONICS AND VOLCANISM

The complete volcanism program was presented at the Nuclear Regulatory Commission (NRC) geology review meeting. Topics emphasized include past work in published papers, work completed since printing of the report on volcanic hazard studies and current areas of uncertainty in the volcanic hazard studies. The NRC position paper on tectonics was reviewed with respect to volcanism. Three topics identified in the position paper are not covered by current volcanism studies: secondary effects of volcanism, relationship of volcanism patterns to seismotectonic models for the southern Great Basin, and relationship between the site of thermal waters and recent volcanism. The latter topic was judged insignificant for the Yucca Mountain site. Trace-element data for basalts of the NTS region were entered into a data base management system in two groups. Sites of hydrovolcanic activity were identified in the southern Great Basin in preparation for field work.

TUFF LABORATORY PROPERTIES

During this quarter, test #TC8 was completed on tuff of Calico Hills from Drill Hole USW G-4. The history of this test is shown in a detailed figure. During the test run of 447 hours, the applied stress was varied from 32 to 40 MPa (with one unplanned excursion to 24 MPa).

SEALING MATERIALS EVALUATION

Concretes are being proposed as a major type of sealing material for the possible nuclear waste repository in Yucca Mountain. Different concretes have been evaluated to address the question of chemical compatability between concrete and tuff host rock. The concretes have been modified to increase chemical compatability primarily by adding silica or silica-rich components. High compressive strengths and low permeabilities have been achieved. When high-pressure/high-temperature experiments were conducted with Well J-13 water, tuff, and concrete, the pH values were initially high. As equilibration is approached, pHs similar to those of the initial Well J-13 groundwater were achieved. The solutions have somewhat lower levels of magnesium and sodium and higher levels of Si and SO_4^{2-} than Well J-13 water does.

EXPLORATORY SHAFT

Technical Direction - Design

Los Alamos personnel worked with the Exploratory Shaft Test Plan (ESTP) Committee to coordinate the design and construction effort with the Exploratory Shaft (ES) testing effort. The quality assurance (QA) level assignments and the rationale for these assignments are being prepared for each of the ES activities, components, and systems.

Test Plan

A major milestone was achieved by the ESTP committee this quarter: the working draft of the test plans for the ES at Yucca Mountain was submitted on November 28, 1983, at the Technical Project Officer (TPO) meeting to NVO-WMPO (Nevada Office of the Waste Management Program Office) and NNWSI TPOs for review.

Integrated Data System

Work this quarter focused on completion of the Integrated Data System (IDS) portion of the ESTP and on procurement actions for the IDS development system.

QUALITY ASSURANCE

Los Alamos

A QA preaward survey was performed at Hewlett-Packard in Cupertino, California.

Comments on the Holmes and Narver NNWSI Records Management study were transmitted to WMPO.

A presentation was made to D. Vieth on ES QA levels.

Several QA training sessions were held for Los Alamos NNWSI personnel.

US Geological Survey

A surveillance schedule of USGS activities was prepared, and surveillance of the Drill Hole UZ-1 instrument installation and stemming operations was performed.

Twelve technical procedures were prepared, reviewed, and submitted for approval signatures.

I. INTRODUCTION

The purpose of the US Department of Energy (DOE) National Waste Terminal Storage (NWTS) program is to safely dispose of the growing quantities of nuclear waste in an environmentally acceptable manner. Substantial accumulations of highly radioactive wastes that already exist and those to be generated in the future must be isolated from the biosphere. The DOE has determined that a safe and feasible method is to store them in mined geologic repositories. Mined repositories can be inspected and monitored, and waste retrieval is possible in the future if desired.

The Nuclear Waste Policy Act of 1982 (Public Law 97-425) reflects a decision to develop geologic repositories for the disposal of these high-level radioactive wastes and spent nuclear reactor fuel. The Act spells out the procedures by which sites will be nominated, characterized, and recommended for development as repository sites. For several years, the DOE has been conducting investigations of potential repository sites in various parts of the nation. In accordance with the Act, the Secretary of Energy will nominate at least five suitable sites for such a repository. Each nomination will include a detailed statement of the basis for the nomination and a detailed environmental assessment of the probable impact of the planned site's characterization activities and what can be done to mitigate potentially adverse conditions.

The NNWSI, which are a part of the NWTS program, include site and regional studies of the Nevada Test Site (NTS) area. These studies will establish whether a technically acceptable site exists there for a repository. The NNWSI program, managed by the DOE Nevada Operations Office, includes scientists and engineers from many fields and organizations, including Los Alamos National Laboratory, Sandia National Laboratories, Lawrence Livermore National Laboratory, US Geological Survey, Westinghouse Electric Corporation, and Science Applications, Inc. The Nevada site is on and adjacent to the NTS in Nye County at a location known as Yucca Mountain (see Fig. 1). The NNWSI participant organizations are conducting investigations to establish the geochemical, geologic, and hydrologic conditions and history of Yucca Mountain and its regional setting. They also are developing engineering criteria for designing and assessing the performance of waste package and repository systems under the conditions present at Yucca Mountain.

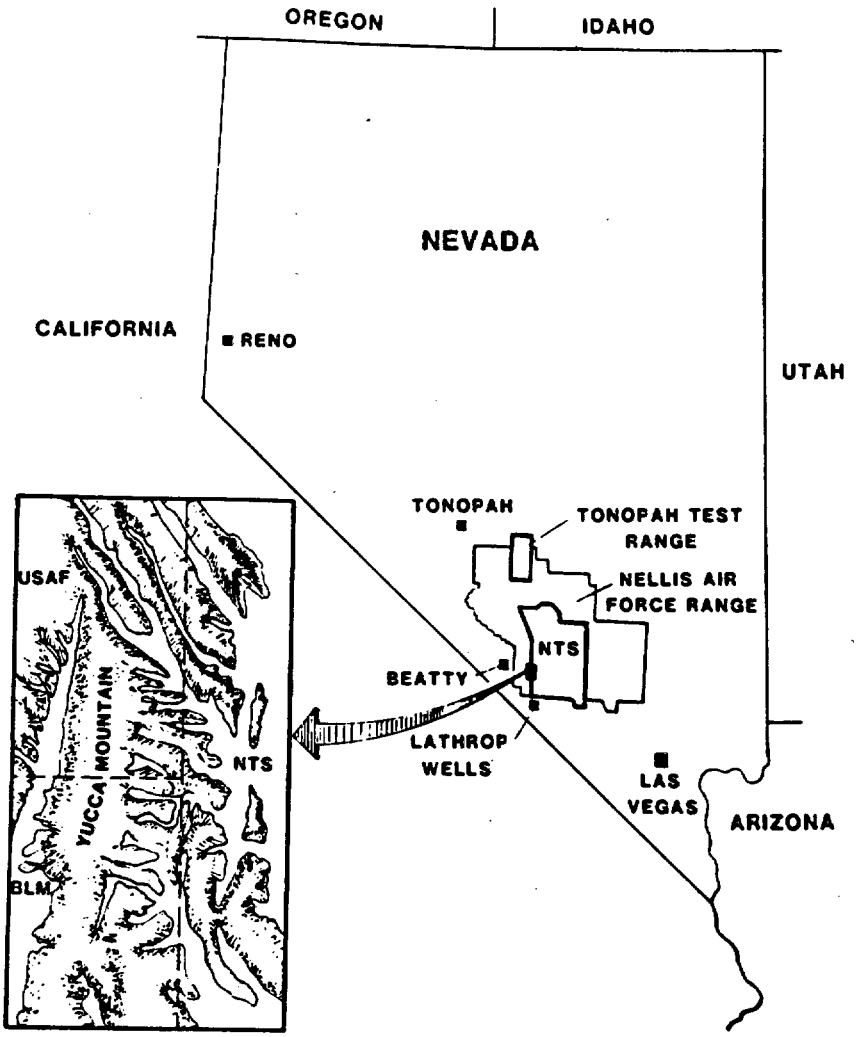

Fig. 1. Yucca Mountain straddles the southwest boundary of the NTS about 100 miles northwest of Las Vegas, Nevada.

Los Alamos National Laboratory's main contribution to these investigations is the study of the geochemistry and mineralogy/petrology of Yucca Mountain and its environs and the engineering design for the exploratory test shaft. This shaft will be mined into the mountain as a first step in a detailed examination of the geology and geochemistry of the repository site.

Many of the rocks in Yucca Mountain have properties that will retard the transport of any radionuclides that might be released from the waste packages. The mineralogy-petrology program will provide a description of rock and fracture-fill petrology and mineralogy in the host rock and along the

transport pathways to the accessible environment. The geochemistry program will quantify the extent of the interactions of radionuclides with the hydrogeological system. These programs provide the basis for a reliable assessment of the rate of transport of radionuclides from the repository to the accessible environment. The program is defined in terms of eight tasks: groundwater chemistry, natural isotope chemistry, hydrothermal geochemistry, solubility determination, sorption and precipitation, dynamic transport processes, retardation sensitivity analysis, applied diffusion, mineralogy and petrology, and quality assurance. Three closely related projects also being conducted at Los Alamos are the study of tectonics and volcanism in the vicinity of NTS, the evaluation of various materials for use in sealing the entrance holes to the repository, and a study of the response of Yucca Mountain rocks to stress under hydrothermal conditions.

II. GEOCHEMISTRY

A. Groundwater Chemistry (A. E. Ogard)

The pumping test in Well USW H-3 was started this quarter. The objectives of this pumping test are threefold: (1) to determine composition of formation water from a test hole in the southern part of the repository block, (2) to obtain formation water from a zone with low permeability, and (3) to obtain additional data for determining transmissivity of a selected interval in USW H-3. The packer that was in place to monitor water levels above and below the packer was removed. An external casing packer with a 3.0-ft-long seal was installed at 2694 to 2697 ft (821 to 822 m) below the ground surface (or ~225 ft below the water table). A Moyno 14 stage 3 pump was installed on 2-7/8-in.-o.d. tubing at 3000 ft (914 m) below the ground surface. This pump is a low-volume rotary pump with a chrome-plated steel rotor inside a Buna-N lined stator. The shape of the rotor and matching stator is very similar to an Archimedes water screw. To keep the friction and wear to a minimum, the rotating sucker rods connecting the rotor to the motor above ground are centered in the 2-7/8-in.-o.d. tubing by Teflon guides.

The pump produced water at a rate of 2.3 gal./minute when first started. Because excess torque developed from drag somewhere in the system, the pump was shut down after a short period and was pulled out for inspection to determine the cause of the drag. The match in length between the stator

string and the rotor string was incorrect. Consequently, the rotor rested on the bottom stop pin of the pump and caused the excess torque. A replacement pump was installed in the well and will be used for the test.

B. Natural Isotope Chemistry (K. Wolfsberg and A. E. Norris)

A contract has been negotiated for services to determine the infiltration profile of the ^{36}Cl bomb pulse at Yucca Mountain and to interpret the data for hydrologic infiltration rates. A large amount of ^{36}Cl, 3 orders of magnitude above natural background level, was injected into the stratosphere by weapon tests in the Pacific between 1952 and 1958. This injection resulted in a pulse of global fallout between 1953 and 1964. This tracer pulse has been used for hydrologic studies of recent water movement, including a study of transit and recharge rates in an arid region. An ultrasensitive technique employing a tandem-accelerator mass spectrometer must be used to detect the 300 000-year ^{36}Cl nuclide. Samples will be taken from four locations (alluvium and fractured tuff) on Yucca Mountain or in its washes, and chloride and ^{36}Cl profiles will be measured to depths of a few meters.

The purchase order was submitted on August 4, 1983, and technical evaluation of the bids was submitted to the Los Alamos R&D contracts group on September 15. The negotiations were completed in December 1983.

C. Hydrothermal Geochemistry (C. J. Duffy)

The stability of the zeolites clinoptilolite and mordenite is very important in siting a nuclear waste repository within Yucca Mountain because the sorptive capacity of the tuff would be reduced by the possible breakdown of these minerals. Smyth's review of the literature[1] suggests that clinoptilolite is probably stable in the environment of Yucca Mountain to about 100°C. Experimental evidence[2,3] indicates that the stability field for mordenite extends to higher temperatures than that for clinoptilolite. If this is true, clinoptilolite and mordenite should not be destabilized by the thermal pulse resulting from emplacement of a repository.

This analysis does not take into account the possible effects of the chemical potential of SiO_2 on the stability of these zeolites. Clinoptilolite and mordenite are generally formed as alteration products of silicic volcanic glass and commonly coexist with cristobalite. They generally do not

exist where the dominant silica phase is quartz. These two patterns are observed in Yucca Mountain.[4,5] When hydrothermal synthesis of clinoptilolite and mordenite was achieved in the laboratory,[6,7] starting materials had been used to provide a chemical potential of SiO_2 higher than that in equilibrium with quartz.

In the field, clinoptilolite and mordenite are replaced by analcime and or feldspars. Such a reaction for sodium end-member clinoptilolite is

$$NaAlSi_5O_{12}\cdot 4H_2O = NaAlSi_3O_8 + 2SiO_2 + 4H_2O \quad ,$$

where clinoptilolite goes to albite plus silica plus water. The aluminum-to-silicon ratio in the clinoptilolite may vary slightly, but the breakdown of clinoptilolite to albite will always produce excess silica. Even more excess silica will be produced if the breakdown is to analcime, and the same is true for the breakdown of mordenite. In consequence, clinoptilolite and mordenite are more likely to be stable in systems in which the chemical potential of silica is higher (such as when it is controlled by rhyolitic glass or cristobalite) than in systems in which it is lower (as it would be if it were controlled by quartz).

These observations suggest that clinoptilolite and mordenite may be stable in Yucca Mountain only where the chemical potential of silica is metastably high. Because metastable phases such as glass and cristobalite provide the only means for maintaining the high chemical potential of silica, this potential must eventually fall to a value in equilibrium with quartz as the mountain moves toward overall equilibrium and quartz becomes the predominant silica phase.

To further examine the effect of the chemical potential of silica on zeolite stability, phase diagrams as functions of log aqueous silica concentration vs log of K^+/H^+ and Na^+/H^+ ratios have been generated. These diagrams are based on the EQ3/6 data base with estimated data for end-member potassium and sodium clinoptilolite.[2] Figures 2 and 3 show the results of these calculations at 100°C. The diagrams at 25 and 200°C are very similar. These diagrams indicate that clinoptilolite is stable at temperatures at least to 200°C if the chemical potential of silica is above that in equilibrium with cristobalite and somewhat lower in the potassium system, and if K^+/H^+ or Na^+/H^+ is sufficiently high. At no temperature is clinoptilolite

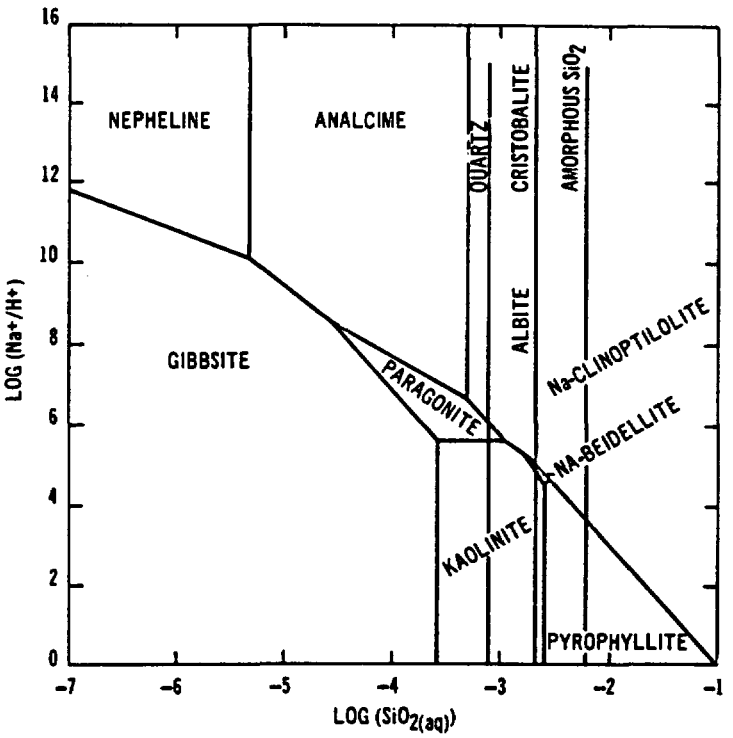

Fig. 2. Phase relations in the system Na_2O-Al_2O_3-SiO_2-H_2O as a function of log(activity of Na^+/activity of H^+) vs log(activity of aqueous SiO_2) at 100°C.

stable at the chemical potential that is determined by equilibrium with quartz. High pH and high chemical potential of silica appear to favor clinoptilolite stability. Although these diagrams are moderately uncertain because the free energy for clinoptilolite had to be estimated, they suggest that clinoptilolite is stable in equilibrium with cristobalite but not with quartz.

Because cristobalite is metastable with respect to quartz, it will tend to transform to quartz. To investigate the possible rate of this transformation, a kinetic model for the transformation has been constructed, based upon

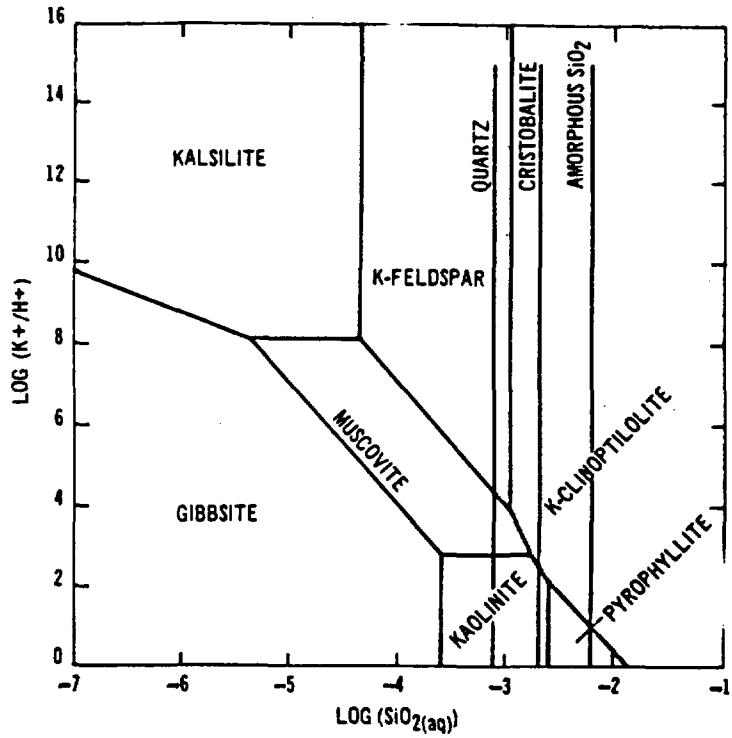

Fig. 3. Phase relations in the system K_2O-Al_2O_3-SiO_2-H_2O as a function of log(activity of K^+/activity of H^+) vs log(activity of aqueous SiO_2) at 100°C.

the data of Rimstidt and Barnes.[8] The dissolution rate for cristobalite (suffix C) is given by

$$dn_{H_4SiO_4}/dt = A_c(k_{c+}a_c a_{H_2O} - k_{c-} a_{H_4SiO_4}) \quad , \qquad (1)$$

where n is the number of moles, t is time in seconds, a is activity, and k_{c+} and k_{c-} are rate constants for dissolution and precipitation, respectively, of cristobalite. The relative interfacial surface area of cristobalite A_c is defined by

$$A_c = A_c^*/A^\circ \quad ,$$

where A_c^* is the surface area of cristobalite in square meters, and A° is 1 m^2. It will be assumed that quartz, cristobalite, and water are all pure phases with activity equal to 1. The activity coefficient for H_4SiO_4 is also assumed to be 1. Equation (1) then becomes

$$dn_{H_4SiO_4}/dt = A_c(k_{c+} - k_{c-}\, m_{H_4SiO_4}) \quad . \tag{2}$$

The relative mass of water in the system M is defined by

$$M = M^*/M^\circ \quad ,$$

where M^* is the mass of water in kilograms, and M° is 1 kg. The molality of H_4SiO_4, $m_{H_4SiO_4}$ can then be expressed by

$$m_{H_4SiO_4} = M^\circ n_{H_4SiO_4} \quad .$$

Calculations will be done on systems containing 1 kg of water. For this case, Eq. (2) becomes

$$dn_{H_4SiO_4}/dt = A_c(k_{c+} - k_{c-}\, n_{H_4SiO_4}) \quad .$$

Because the number of moles of H_4SiO_4 produced must equal the number of moles of cristobalite dissolved,

$$dn_c/dt = -A_c(k_{c+} - k_{c-}\, n_{H_4SiO_4}) \quad . \tag{3}$$

Similar equations hold for quartz.

For a system of both quartz (suffix q) and cristobalite in 1 kg water,

$$dn_{H_4SiO_4}/dt = A_q(k_{q+} - k_{q-}\, n_{H_4SiO_4}) + A_c(k_{c+} - k_{c-}\, n_{H_4SiO_4}) \quad .$$

The equations for dn_c/dt and dn_q/dt use the form of Eq. (3).

To solve for $n_{H_4SiO_4}$, n_q, and n_c as a function of time, A_q and A_c must be expressed as functions of n_q and n_c. The assumption has been made that quartz and cristobalite are present as cubes with constant edge dimension E. For cubes,

$$V = A^*E/6 \quad ,$$

where V is the volume of the cubes. Noting that

$$n = V/\bar{V} \quad ,$$

where $\bar{V}$ is the molar volume,

$$A^* = 6n\bar{V}/E \quad ,$$

and

$$A = 6n\bar{V}/A^\circ E \quad .$$

For E in centimeters,

$$A_q = 1.36 \cdot 10^{-2} n_q/E \quad ,$$

and

$$A_c = 1.54 \cdot 10^{-2} n_c/E \quad .$$

For a saturated rock with porosity P and x_q volume per cent quartz and x_c volume per cent cristobalite, the volume of rock V_r that will hold 1 kg of water, assuming a water density of 1 g/cm^3, is expressed by

$$V_r = 10^3/P \quad (cm^3) \quad .$$

The volume of minerals V_m present is given by

$$V_m = 10^3(1-P)/P \quad (cm^3) \quad ,$$

and the number of moles of quartz and cristobalite in this volume are

$$n_q = 10^3 x_q(1-P)/P\bar{V}_q$$

and

$$n_c = 10^3 x_c(1-P)/P\bar{V}_c \quad .$$

This model assumes that cristobalite is transformed to quartz only by dissolution and precipitation and that no solid-to-solid transition occurs. Further, it is assumed that the rate is determined by the rates of dissolution and precipitation and not by the rate of transfer in the fluid phase.

In performing the calculation, it is necessary to start with a finite quantity of quartz because the model does not provide for nucleation. Calculations starting with 0.25% quartz and 50% cristobalite have been performed for a rock with 10% porosity. This corresponds to starting conditions of 1 mole of quartz and 175 moles of cristobalite per kilogram of water. Because of the relationship assumed between the relative interfacial surface area A and the crystal edge E, the time t required for the system to reach a given state is directly proportional to E. Calculations were performed at 35, 50, 100, and 150°C. The time at which the silica in solution began to drop significantly as a result of quartz precipitation is expressed by

$$\log(t/E) = 14.8 - 0.025T \quad ,$$

where t is the time in years, E is in centimeters, and T is in degrees Kelvin. The time at which only insignificant cristobalite remained is given by

$$\log(t/E) = 15.8 - 0.026T \quad .$$

The cristobalite in Yucca Mountain is quite fine grained. Most of the grains are ~1 μm in average dimension. If they are assumed to be 10-μm cubes, it would almost certainly be an underestimation of the surface area. The model predicts that 10-μm grains of cristobalite will persist less than 10^5 years at 35°C. This is clearly not the case in Yucca Mountain, where much of the cristobalite has probably been present ~10^7 years. Persistence

of cristobalite might be enhanced as a result of the lack of nucleation of quartz or the lack of an effective fluid phase for transporting aqueous silica. With the exception of the upper Topopah Spring Member and higher members, quartz is present in most of the Yucca Mountain tuffs in both the saturated and unsaturated zones. It is extremely unlikely that this quartz has all formed in the very recent past. Therefore, the lack of quartz nucleation seems an unlikely explanation for the persistence of cristobalite. It seems much more likely that where cristobalite is present, its transformation to quartz is retarded by the lack of a continuous fluid phase, or, where the fluid phase is continuous, transport of silica in the fluid controls the rate of transformation.

D. Solubility Determination

1. Americium Thermodynamic Data (J. F. Kerrisk)

A thermodynamic data file for americium has been completed for the EQ3/6 chemical equilibrium program. Data were found for 26 aqueous species and 3 solids. In addition to the information discussed in the previous quarterly report,[9] recent results for the solubility of $Am(OH)CO_3$ (Ref. 10) have been included. There is still considerable uncertainty about the identity and formation constants of aqueous americium complexes with carbonate. At this time, only 25°C data are available for essentially all americium species; however, data for americium at higher temperatures for important complexes and solids may be required for a thorough understanding of americium behavior.

The solubility of americium in water that is characteristic of Yucca Mountain was calculated using the compiled thermodynamic data. Analyses of water from Well J-13 were used to define the water composition.[11] The observed pH of Well J-13 water is approximately 7, and the total carbonate is 2.3×10^{-3} M. The Eh was assumed to be 400 mV; this assumption should not affect the results because only the Am(III) oxidation state is expected in dilute, near-neutral solutions. The solid controlling solubility was assumed to be $Am(OH)CO_3$. At pH 7, the solubility was 1.0×10^{-8} M; at pH 8, the solubility had decreased to 1.2×10^{-9} M. In the pH range from 7 to 8, $AmCO_3^+$ is the predominant aqueous species. Solid $Am_2(CO_3)_3$ was also near saturation under these conditions, but the formation constant for this species has only been estimated. Solid $Am(OH)_3$ was undersaturated; however, it could control

solubility at higher pH or lower total carbonate content. (A draft report describing the americium thermodynamic data and solubility calculations has been completed and will be issued as a Los Alamos Laboratory report.)

2. Plutonium Chemistry in Near-Neutral Solutions (D. E. Hobart, T. W. Newton, and V. L. Rundberg)

A study of the rates of disproportionation and the first steps in the polymerization of Pu(IV) has been completed; a paper describing this work was presented at the Seventh International Symposium on the Scientific Basis for Nuclear Waste Management.[12] The rates of polymerization and disproportionation of Pu(IV) have been studied using low concentrations: (1.7 - 10) x 10^{-6} M Pu, (0.8 - 12) x 10^{-4} M HCl, and 0.01 M ionic strength. Unreacted Pu(IV) was determined as a function of time by a chemical method that is based on two facts: (1) Pu(IV) reacts rapidly with Os(II) complexes such as the tris-4,4'-2,2'-bipyridine complex and (2) the complexes react slowly, if at all, with the Pu(IV) polymer and the products of the disproportionation reaction, Pu(III) and Pu (V). These two oxidation states are determined by using their reaction with Ce(IV) sulfate. At constant pH, $-d[Pu(IV)]/dt = k'[Pu(IV)]^2$. Log k' varies from about 4.25 at pH 3 to about 7.0 at pH 4.1 (units for k' are $M^{-1}min^{-1}$). The H^+ dependence varies from about -2 to -3 over the pH range studied. The measured rate is the sum of those for polymerization and disproportionation; the latter reaction amounts to about 0.75 of the total at pH 3 and only 0.20 at pH 4. If this trend continues to higher pH, disproportionation may be insignificant in the pH range 7 to 8, which is characteristic of water at Yucca Mountain. The second-order rate constants for disporportionation are very much larger than were expected on the basis of extrapolation from 0.2 to 1.0 M $HClO_4$ solutions. The products of the reaction do not affect the rate, but U(VI), aged Pu(IV) polymer, and CO_2 increase the rate.

The disproportionation of Pu(V) in near-neutral solutions is being investigated because the equilibrium constant for the reaction

$$2PuO_2^+ = PuO_2 \cdot nH_2O_{(solid)} + PuO_2^{2+} \quad , \qquad (4)$$

with the appropriate standard potentials, leads to a value for the solubility product for $PuO_2 \cdot nH_2O_{(solid)}$. Previous attempts to study the "reproportionation reaction" at Los Alamos were unsuccessful because alpha-reduction of the $^{238}Pu(VI)$ reactant was faster than the chemical reaction to form Pu(V). However, recent work at Oak Ridge National Laboratory showed that at fairly high Pu concentrations (10^{-2} M), the reaction above [Eq. (4)] proceeds to give PuO_2^{2+} and the polymer of Pu(IV) (Ref. 13).

The Pu(V) solutions have been prepared electrolytically and Pu(V) disproportionation reactions have been monitored spectroscopically at various pH values. The reaction appears to approach a steady state in about 20 days. Solids that formed have been collected and analyzed by x-ray powder diffraction, and preliminary data confirm the formation of PuO_2 polymer. The supernatant is analyzed by recording the absorption spectrum of the major Pu(VI) peak; the Pu(V) is oxidized by Ce(IV), and the increase in the absorbance . Pu(VI) reflects the initial Pu(V) present. [The Pu(IV) polymer reacts very slowly with Ce(IV)]. The parameter that can be directly obtained is the equilibrium constant for reaction (4);

$$Q' = \frac{(PuO_2^{2+})}{(PuO_2^{+})^2} \quad .$$

The provisional Q' values determined from the present work are in close agreement with those of Madic et al.[13] and correlate with other literature sources.[14,15] The effects of radiolysis on reaction (4) will be investigated using lower specific activity ^{242}Pu rather than the presently employed ^{239}Pu.

3. Determination of Solubilities and Complexation of Waste Radionuclides Pertinent to Geologic Disposal (H. Nitsche, Lawrence Berkeley Laboratory, and A. E. Ogard)

In the event that the canister and waste form fail to contain radioactive waste materials, radionuclides will enter the local groundwater system. The radionuclides will react with various components of the groundwater, dissolved waste-form materials, and the host rock to form insoluble compounds and solution species that can provide major controls on the solution concentrations and migration rates of the waste radionuclides.

Precipitation of stable solid phases will retard the migration of radionuclides relative to the average velocity of groundwater; on the other hand, formation of aqueous complexes will tend to reduce this retardation effect.

This is a new program started November 1, 1983; its objective is to identify and obtain appropriate data on the solubilities of compounds and on solution complexes of the important waste radionuclides likely to form in groundwater systems. Information on the site-specific geochemical behavior of the waste radionuclides of concern is needed for site characterization and to demonstrate that the expected performance of the repository site will be in compliance with technical criteria stated in Federal Regulation 10CFR60.[16]

Work was initiated to measure the solubilities of NpO_2^+, NpO_2^{2+}, Pu^{4+}, PuO_2^+, PuO_2^{2+}, and Am^{3+} individually, in groundwater from the NTS, and in aqueous $NaClO_4$ solutions of similar pH and ionic strength. This investigation is intended to be a survey to compare the solubilities and oxidation state distribution of neptunium, plutonium, and americium in the NTS groundwater with a noncomplexing aqueous solution. The results should help decide the direction of future measurements.

a. Preparation of Stock Solutions. A purified $^{237}NpO_2^+$ standard solution was prepared. Three portions of NpO_2 were dissolved in 8 M HNO_3 containing a trace of NaF to facilitate the dissolution. The neptunium was then precipitated as the hydroxide with NaOH. After it was washed, the precipitate was dissolved in 0.1 M HNO_3, and the neptunium was reduced to the +3 state by contacting the solution with zinc amalgam. Purging the resulting solution with air for a few minutes converted all the neptunium to the +4 oxidation state. The neptunium was then purified in the tetravalent state by anion-exchange chromatography. The anion-exchange column was prepared with 100 to 200 mesh Biorad AG 1 x 8 resin. Loading and washing was done with 8 M HNO_3, and elution was done with 0.3 M HNO_3. The eluates were fumed twice with concentrated $HClO_4$ to near dryness. The residue was then redissolved in 10 mℓ of 0.1 M $HClO_4$. Alpha counting and microtitration with EDTA[17] were used to standardize the stock solution. The standardized solution (identification code Np-237-11-29-83) is $1.171 \approx 0.034 \times 10^{-1}$ M. Spark emission spectroscopic analysis of the standardized solution showed only the contaminant magnesium, 0.03% by weight, above detection limits.

Pure ^{242}Pu oxide, obtained through the National Production Program from Oak Ridge (Batch No. Pu-242-207AR2), was dissolved in 6 M HCl. Conversion to

the perchlorate was made by fuming to near dryness twice with concentrated $HClO_4$. The residue was taken up in 1 M $HClO_4$. Spark emission spectroscopic analysis showed only calcium, 0.01% by weight, above detection limits. The concentration of the acidified stock solution (4.2×10^{-2} M) was determined from the results of gross alpha-counting of dried aliquots with a gas proportional counter and liquid aliquots with a Packard 400C liquid scintillation counter. The results of a mass spectroscopic analysis, supplied by Oak Ridge, of the original PuO_2 indicated the following isotopic composition: ^{238}Pu (0.003%), ^{239}Pu (0.018%), ^{240}Pu (0.083%), ^{241}Pu (0.096%), ^{242}Pu (99.80%), and ^{244}Pu (<0.0005%) by weight. Alpha pulse height analysis gave roughly the same percentages for the ^{242}Pu, ^{239}Pu, and ^{238}Pu. Because the plutonium solubility in natural groundwaters is expected to limit solution concentrations to the 10^{-8} M range (Refs. 18 and 19), the specific alpha activity of the stock solution will be increased by the addition of ^{238}Pu. This will facilitate concentration measurements by liquid scintillation counting.

The americium used to prepare a stock solution was obtained through the National Heavy Element Production Program from Oak Ridge. Unfortunately, this was an old sample, and its original batch number was unknown. The americium was cleaned of soluble salts by two NaOH precipitation-dissolution cycles. The resulting tan-colored $Am(OH)_3$ was then dissolved in 1 M HCl. A greyish residue remained and was leached twice with 1 M HCl to remove the remaining americium. The leach solutions were combined, taken to dryness, and redissolved in 0.05 M HCl. Alpha pulse height analysis indicated that the sample was 88.39% ^{243}Am, 1.95% ^{241}Am, and 11.66% ^{244}Cm by activity. The americium was separated from the curium, and other cations were separated by cation-exchange chromatography using Biorad AG 50 x 12 resin (~400 mesh). The resin was converted to the NH_4^+ form by washing with 1 M NH_4-α-hydroxyisobutyrate (NH_4BUT) (pH = 4.05) and conditioned with 0.4 M NH_4-BUT (pH = 4.05). Approximately 4 mg of americium was loaded onto the column in 0.05 M HCl, and the elution was made with 0.4 M NH_4-BUT (pH = 4.05). Analysis by alpha pulse height indicated that the isotopic composition of the americium fraction from the column was 97.53 and 99.87% ^{243}Am, 2.15 and 0.13% ^{241}Am, and 0.32 and 0.0008% ^{244}Cm by activity and weight, respectively.

A final purification and separation from the NH_4-BUT was accomplished by cation-exchange chromatography on Biorad AG 50 x 8 resin. The column was

loaded with the 0.05 M HCl solution containing the americium and was washed with 3 column volumes of 0.05 M and 2 M HCl; the americium was eluted with 6 M HCl. The americium fraction was standardized by gross alpha counting and identified as Am-243-12-20-83. Spark emission spectroscopic analysis is being performed.

b. Preparation of Oxidation States. The various oxidation states of plutonium and neptunium required will be obtained by electrochemical techniques. Controlled-potential coulometry for both elements is discussed in depth in the literature.[20-23] Our coulometric cell is a three-electrode set up. The electrodes consist of a platinum wire counter electrode, a Ag/AgCl/3 M NaCl reference electrode and a platinum gauze working electrode. The counter and reference electrodes are separated from the analyte solution by Vicor fritted salt bridges that contain 1 M $HClO_4$. Solution purging or blanketing with argon is accomplished through a port in the cell top. The solution is stirred with a magnetic spinbar.

The purity of each valence state is established by absorption spectroscopy using a Cary Model 17 recording spectrometer. A MINC II-B (LSI-11/2) minicomputer interfaces with the spectrometer and allows digital data collection and manipulation (for example, background subtraction and data smoothing). Cuvettes are 100 mm in path length and 5 mℓ in volume. A 1 M $HClO_4$ solution is used in the reference cell. Characteristic absorption bands and molar absorptivities are listed below. The absorptivity values for PuO_2^+ listed in Table I are taken from the literature[24] and are being verified spectroscopically.

The neptunium in the stock solution is in the 6+ state. It is reduced completely to NpO_2^+ at 645 mV (AgCl).

The plutonium in the stock solution is almost completely PuO_2^{2+} after the fuming procedure. The reduction of PuO_2^{2+} to Pu^{4+} cannot be performed directly. Because of the irreversibility of the reaction PuO_2^+ to Pu^{4+}, a large overpotential must be applied. This leads to the formation of Pu^{3+}. Therefore, all PuO_2^{2+} is reduced at 580 mV (vs AgCl) or lower to Pu^{3+}, and then it is oxidized at 940 mV (AgCl) to Pu^{4+}. Likewise, because of the irreversibility of the Pu^{4+} to PuO_2^+ oxidation reaction, PuO_2^+ can only be prepared by reducing hexavalent plutonium solutions at 645 mV (vs AgCl). Cohen[20] prepared 97% PuO_2^+ solutions from PuO_2^{2+} in 0.2 M $HClO_4$ by reduction at 10°C; this procedure is being tested.

TABLE I

ABSORPTIVITY VALUES

Oxidation State	Wave Length (nm)	$\varepsilon(M^{-1}cm^{-1})$
Pu^{4+}	470	51
PuO_2^+	(1130,563)	(22,20)
PuO_2^{2+}	830	555
NpO_2^+	980	395
NpO_2^{2+}	1223	44

c. Equipment. The items for the solubility measurement system have been obtained, and assembly is nearly complete. The solubility measurements using $NaClO_4$ will be made in a Model HE-43-2 inert-atmosphere box to avoid contamination of solutions by CO_2. Experience indicates that substantial drifts in pH can occur in even 24-hour periods in poorly buffered solutions. Because the solubility measurements in $NaClO_4$ at pH ~7 are of this type, pH control using a pH-stat is needed.

A CCM Laboratory Data Control Computer system is used to sense any one of six pH electrodes (Beckman Model 39505) through an Orion model 605 pH-electrode switch (modified for remote control) and a Radiometer model pHM 84 pH meter. If the pH of the selected solution is not within the preselected range, a small volume (typically a few microliters) of dilute acid or base is dispensed on computer command to the appropriate solution through a computer-selectable, six-position Eldex model SV-1062 solvent delivery valve by a Hamilton model 100000 digital diluter. All solutions are continuously monitored and pH corrections are made as required. The Hamilton Diluter, associated electronics, and acids and bases are contained in a Labconco controlled-atmosphere box (under argon) adjacent to the inert box to avoid radioactive contamination. The CO_2 contents of the box atmospheres are determined with a Gow-mac model 69-750p gas chromatograph.

4. Colloids (J. L. Thompson)

Recently, experiments have been initiated to better characterize the actinide species used in Los Alamos laboratory sorption measurements. In

particular, these experiments will determine whether colloidal species with diameters less than 50 nm are present initially or forming in the feed solutions employed for our sorption studies. In the first series of experiments, the response of americium solutions (suspensions?) to multiple filtrations has been observed under a variety of conditions. The americium was prepared in Well J-13 groundwater by the standard procedure; initially the americium concentration was about 10^{-7} M in air-equilibrated water at room temperature. The solutions were repetitively filtered over a period of several weeks using 400- or 50-nm Nuclepore polycarbonate filters. It became apparent that sorption of americium on all surfaces contacted by the liquid accounted for most of the losses in the repetitive filtrations. Sorption effects were demonstrated using filters with punctures (so that no filtration occured) and a solution about 0.2 M in $HClO_4$, from which sorption was considerably enhanced. Observations to date indicate that some filterable species (that is, larger than 50 nm in diameter) may form when solutions 10^{-7} to 10^{-9} M in americium are aged for several days. However, evidence for this behavior is ambiguous because sorption also increases with these aged solutions. Research in this area will continue, especially with more dilute solutions.

E. Sorption and Precipitation

1. Batch Sorption Experiments of Sorption and Precipitation

(F. O. Lawrence, S. D. Knight, M. R. Cisneros, and K. W. Thomas)

Studies continued in the investigation of the sorptive behavior of Yucca Mountain tuffs. Sorption and desorption ratios measured this quarter are reported in Table II. The tuff samples studied are described in the previous quarterly report,[9] except sample GU-4-1502. The x-ray analysis reveals that this tuff is 57 ± 10% clinoptilolite, 9 ± 4% mordenite, 7 ± 2% quartz, 5 ± 2% cristobalite, and 23 ± 10% alkali feldspar.

2. Long-Term Sorption Experiments on Technetium and Neptunium

(S. D. Knight, F. O. Lawrence, M. R. Cisneros, and K. W. Thomas)

Sorption ratios for technetium on tuff samples studied to date are zero or nearly zero at contact times of 3 to 6 weeks.[11,25] Neptunium sorption ratios are greater than zero but typically less than 10 (Refs. 11, 25, 26). Long-term experiments have been undertaken to determine if the measured sorption ratios for these two elements increase or, in the case of neptunium,

TABLE II

SORPTION VALUES FOR SORPTION EXPERIMENTS

Core[a]	Element	Traced Feed (pH)	Traced Feed Concentration (M)	Sorption Time	Sorption Ratios (mℓ/g) Experimental Value (pH)		Sorption Ratios (mℓ/g) Average Value[b] (pH)	Desorption Time	Desorption Ratios (mℓ/g) Experimental Value (pH)		Desorption Ratios (mℓ/g) Average Value[b] (pH)
GU3-916	Np	---	6×10^{-11}	6 weeks	4.8 (8.76)	4.9 (8.65)	4.9 (1)	6 weeks	35 (8.76)	32 (8.80)	33 (1)
				3 months	5.1 (8.69)	5.4 (8.68)	5.3 (1)	---			
	Pu	8.42	1×10^{-7}	6 weeks	280 (8.66)	230 (8.66)	250 (25)	6 weeks	720 (8.66)	640 (8.66)	680 (40)
	Tc	8.57	6×10^{-10}	6 weeks	0.50 (8.51)	0.94 (8.57)	0.72 (0.2)		Not Applicable		
				13 weeks	0.33 (8.75)	1.3 (8.70)	0.81 (0.5)				
GU3-1301	Np	8.56	6×10^{-11}	3 months	2.3 (8.63)	2.1 (8.65)	2.2 (1)	6 weeks	23 (8.66)	26 (8.74)	25 (2)
				3 months	2.1 (8.65)	1.9 (8.67)	2.0 (1)	---			
	Tc	8.67	7×10^{-10}	6 weeks	0.058 (8.41)	0.022 (8.47)	0.04 (0.02)		Not Applicable		
				13 weeks	0.065 (8.63)	0.002 (8.69)	0.03 (0.03)				

TABLE II (cont)

Core[a]	Element	Traced Feed (pH)	Traced Feed Concentration (M)	Sorption Time	Sorption Ratios (mℓ/g) Experimental Value (pH)		Sorption Ratios (mℓ/g) Average Value[b] (pH)	Desorption Time	Desorption Ratios (mℓ/g) Experimental Value (pH)		Desorption Ratios (mℓ/g) Average Value[b] (pH)
G4-1502	Np	8.72	1×10^{-10}	6 weeks	4.6 (8.33)	3.5 (8.32)	4.0 (1)	6 weeks	13 (8.71)	10 (8.70)	11 (2)
				3 months	5.1 (8.66)	3.4 (8.70)	4.3 (1)	---			
	Pu	8.65	1.5×10^{-7}	6 weeks	56 (8.72)	62 (8.69)	59 (3.4)	6 weeks	260 (8.69)	190 (8.69)	230 (34)
	Tc	8.74	8×10^{-10}	6 weeks	0.042 (8.60)	-0.003 (8.60)	0.02 (0.02)		Not Applicable		
				13 weeks	0.06 (9.0)	-0.038 (8.81)	0.01 (0.05)				

[a] Fraction size is 75 to 500 μm.

[b] Numbers in parentheses are standard deviations of the mean.

change over periods of time longer than 6 weeks. Three tuff samples are being studied and have been described in the previous quarterly report.[9] Scheduled contact times are 6 weeks and 3, 6, 9, 12, and 15 months. Table II presents the data available to date on long-term neptunium and technetium measurements. It appears that there is little change in measured sorption ratios for neptunium or technetium in tests of up to 3 months.

3. Cation-Exchange Capacity of Tuffs (K. Wolfsberg)

Cation-exchange capacity (CEC) is a measure of the total capacity of a rock to exchange ions without regard to relative strengths that are described by sorption ratios or equilibrium constants. Knowledge of the CEC of rocks along the flow path is important for predicting the quantities of waste elements that can be sorbed. In earlier work,[11] it was shown that knowledge of CEC values for tuff minerals are necessary when correlating sorption ratios with mineralogy. If we assume that the CEC of a rock is the weighted sum of the CEC values of its component minerals, it should be possible to obtain CEC values for individual tuff minerals by using the CEC values for a variety of tuffs of known composition. The replaceable ion (calcium, sodium, etc.) is also obtained from these CEC measurements. This information may be useful in the future for making correlations.

Employing the procedures in Ref. 27, CEC values were determined by the National Soil Survey Laboratory for tuff samples used in Los Alamos sorption studies. The CEC was determined by measuring the quantity of ammonium ion extracted from an ammonium acetate (pH 7.0) solution. This value, given in the column "CEC by NH_4OAc" in Table III, assumes there is a milliequivalent-for-milliequivalent replacement of ammonium ion for those cations in the tuff sample. This may not be strictly true for multivalent ions such as Ca^{+2}. Calcium, magnesium, sodium, and potassium were also determined in the ammonium acetate extract, and the values (normalized to 100%) for these are given also in Table III. For some samples, extractable acidity was determined by an ethanolamine method and the percentage of the CEC by sum cations is presented here.

In principle, then, the CEC is also the sum of the values for extractable bases (calcium, sodium, etc.) and extractable acidity. These values are given in Table III as "CEC by Sum Cations." In general, there is reasonable agreement between the two methods for determining CEC. The disagreement in

TABLE III

CATION-EXCHANGE CAPACITIES[a]

Sample	Particle Size (μm)	CEC by NH OAc (meq/100 g)	CEC by Sum Cations[b] (meq/100 g)	Sum of Bases[c] (%)				Extractable Acidity of CEC (%)
				Ca	Mg	Na	K	
JA-8	75-500	28.4	33.8	81	12	3	4	5
JA-18	106-150	78.7	79.0	29	--	28	42	7
JA-18	355-500	69.8	(75.3)	29	--	28	42	9
JA-26	<75	3.3	9.3	25	4	67	5	9
JA-28	75-500	3.6	4.7	36	3	62	tr	17
JA-32	150-180	2.8	3.3	45	3	39	12	--
JA-32	250-355	2.5	(3.2)	44	3	44	9	
JA-37	<106	26.7	(56.9)	86	5	6	3	
JA-37	150-180	23.8	(49.6)	87	5	5	3	
YM-5	75-500	23.6	29.1	65	29	3	4	5
YM-22	75-500	0.8	5.8	58	16	16	10	47
YM-22	<75	1.4	4.4	48	13	23	18	9
YM-30	75-500	8.7	12.0	70	12	12	6	10
YM-38	<500	151.7	(151.5)	47	0.6	19	33	
YM-38	75-500	122.0	(118.8)	46	0.8	21	33	
YM-42	75-500	52.7	66.3	72	2	15	11	2
YM-45	106-500	5.5	9.5	85	4	5	3	16
YM-46	75-500	3.8	8.9	61	4	18	17	19
YM-48	106-500	46.0	48.4	52	1	33	14	2
YM-49	106-250	111.9	(106.0)	54	2	28	16	
YM-49	75-500	118.7	117.0	58	3	24	15	1
YM-54	75-500	2.3	4.5	93	3	3	3	11
G1-1292	75-500	--	(5.3)	94[d]	2	4	--	
G1-1436	<500	164.6	174.8	11	0.6	46	43	0.3
G1-1854	<75	126.5	(130.0)	19	0.3	52	29	
G1-1854	75-500	104.1	114.9	18	0.3	52	29	0.2
G1-1883	<106	0.5	4.9	46	17	29	7	16
G1-1982	<38	14.5	(22.0)	34	5	52	10	
G1-1982	<500	16.4	7.5	28	3	52	17	5

TABLE III (cont)

Sample	Particle Size (μm)	CEC by NH OAc (meq/100 g)	CEC by Sum Cations[b] (meq/100 g)	Sum of Bases[c] (%) Ca	Mg	Na	K	Extractable Acidity of CEC (%)
G1-2233	<38	55.6	(136.0)	19	0.4	57	24	
G1-2233	<500	88.2	(90.5)	19	0.3	57	23	
G1-2233	106-500	68.6	(70.7)	18	0.1	59	22	
G1-2289	<500	132.4	(144.3)	37	0.1	53	9	
G1-2334	<38	6.8	7.5	64	7	23	7	tr
G1-2334	75-355	5.0	(5.5)	53	2	38	7	
G1-2334	355-500	3.6	(4.2)	60	2	31	7	
G1-2363	<500	4.8	8.0	74	1	25	tr	1
G1-2410	106-500	0.4	4.9	78	--	22	--	--
G1-2476	75-500	0.4	3.8	49	--	41	11	3
G1-2698	<500	116.4	(118.9)	15	0.3	69	15	
G1-2840	<38	6.3	(7.3)	71	4	18	7	
G1-2840	<106	5.1	(6.2)	61	2	31	6	
G1-2840	150-355	3.9	(4.8)	67	tr	29	4	
G1-2840	75-500	0.3	4.3	74	--	24	3	--
G1-2840	355-500	3.4	(3.8)	76	3	16	5	
G1-2854	75-500	0.9	3.8	74	--	24	3	--
G1-2901	<500	0.5		( )[e]	(--)	(1.2)	(0.3)	(--)
G1-3116	<500	23.8	28.4	24	0.4	72	4	0.4
G1-3658	<500	50.8	(57.4)	37	5	57	1	
G2-332	<500	73.6	(78.3)	81[b]	16	1	1	
G2-339	<500	29.8	36.3	79	18	1	2	8
G2-547	75-500	33.7	36.1	76	13	6	5	8
G2-723	<500	9.9		( )[f]	(1.3)	(0.6)	(0.8)	
G2-770	<500	2.9	2.8	40	8	20	32	11
G2-1951	<500	139.1	138.0	48	3	25	25	1
G2-1952	75-500	123.5	124.0	46	0.4	30	23	1
G2-2000	<500	120.9	123.9	50	2	30	18	1
G2-3308	<500	4.2	3.3	47	--	41	13	3
G2-3933	75-500	7.1		( )[g]	(6.2)	(4.1)	(1.0)	
GU3-433	<500	1.9	2.6	35	10	30	25	23
GU3-855	<500	3.1	4.4	45	13	24	18	14

TABLE III (cont)

Sample	Particle Size (μm)	CEC by NH OAc (meq/100 g)	CEC by Sum Cations[b] (meq/100 g)	Sum of Bases[c] (%) Ca	Mg	Na	K	Extractable Acidity of CEC (%)
GU3-855	75-500	2.9	4.5	49	13	21	18	13
GU3-916	75-500	3.1	3.9	38	15	26	21	13
GU3-1203	75-500	2.3	2.3	70	9	13	9	--
GU3-1301	75-500	1.1	1.[illegible]	73	--	18	9	8
GU3-1437	75-500	2.7	2.5	64	--	24	12	--
GU3-1531	75-500	11.9	12.7	77	1	14	8	6
GU3-1937	<500	150.39	149.3	10		54	35	1
G3-3005	<500	3.9		( )[d]	(--)	(1.5)	(0.7)	
G3-4868	<500			( )[e]				
G3-4907	<500	7.1	(11.8)	54	1	40	5	
G4-1502	75-500	157.8	163.8	14	--	46	41	1

[a] Blank = not determined; dash = not detected.

[b] Values in parentheses represent only the sum of bases; extractable acidity was not determined.

[c] Values in parentheses are in meq/100 g.

[d] Trace $CaCO_3$.

[e] 3% $CaCO_3$.

[f] 29% $CaCO_3$.

[g] 1% $CaCO_3$.

some low values of CEC may be the result of (1) dissolution of rock rather than ion replacement, (2) the assumption for multivalency discussed above, or (3) experimental sensitivity. In general, variations with particle size appear to be small, and where variations occur, they have also been observed in sorption studies.[26] This variation is caused by enhancement of the very fine fraction in clays during the sieving process. The CEC values reported for some tuffs previously[26] by exchanging with cesium agree reasonably with those reported here.

Using a multiple-regression least squares program, the CEC values (NH_4OAc) are being evaluated against mineralogy. Preliminary CEC values for clinoptilolite, mordenite, smectite, glass, and illite-muscovite are 2.6 ± 0.2, 1.3 ± 0.6, 1.6 ± 0.3, 0.7 ± 0.2, and 0.7 ± 0.3 meq/g, respectively. Values of 2.3, 2.3, and 1.2 meq/g were used for clinoptilolite, mordenite, and smectite, respectively, in Ref. 26.

4. Microbiological Activity at Yucca Mountain (L. E. Hersman, F. O. Lawrence, S. D. Knight, M. R. Cisneros, and K. W. Thomas)

The organisms first isolated on detergent or polymer media at Yucca Mountain are still being studied. The growth characteristics of such organisms are important because a growing microbial population can produce a change in soil pH and Eh, thereby possibly affecting radionuclide movement. It is further suspected that soil microorganisms provide chelating agents that may also affect the behavior of radionuclides through complexation or precipitation mechanisms. The organisms studied were characterized in an earlier progress report.[2] Current research is focusing on the influence of bacteria and their by-products on the mobility of plutonium and strontium in soils.

Bacteria often serve as surfaces for metal attachment. As bacteria are removed from solution (by centrifugation, precipitation, filtering, etc.), metals attached to the bacteria will also be removed. This phenomena is also being investigated with sorption experiments. Bacteria were isolated from the nonsterile control tubes of a previous experiment, where they were growing in the presence of crushed tuff and groundwater. A mixed culture of these bacteria was inoculated into nutrient broth (Diflo, Detroit, Michigan) and incubated at 25°C for 5 days. Cells were washed twice with, and resuspended in, sterile, de-ionized distilled water. Finally, 1 mℓ of cell

suspension was added to 19 mℓ of a sterile slurry of tuff and water for the batch sorption measurement, using the method described in an earlier report.[9]

The results of this experiment indicate that bacteria may affect plutonium sorption. The sorption ratio for the sterile feed/non-sterile tuff (nonsterile control) was 35 mℓ/g, whereas for the sterile feed/sterile tuff (sterile control) it was 24 mℓ/g. When bacteria were added, the sterile feed/sterile tuff plus bacteria gave an R_d of 120 mℓ/g. The final bacteria counts for these three experiments were 1.7×10^6, 8.5×10^2, and 7.43×10^6 colony-forming units (CFU), respectively. The lowest R_d value and the lowest bacterial count occurred in the same system (24 mℓ/g and 8.5×10^2 CFU). Similarly, the intermediate R_d was found with the next higher bacterial count (35 mℓ/g and 1.71×10^6 CFU), and the highest R_d had the highest bacterial count (120 mℓ/g and 7.43×10^6 CFU). Therefore, it appears that the greater the bacterial count, the greater the measured R_d value. However, this was not substantiated in the next experiment.

A second experiment was performed to analyze the dual effects of growth medium and bacteria on sorption. Detergent and polymer media were inoculated with species No. 8 and No. 9, respectively (see Ref. 2), incubated for 1 week, and diluted to 10^{-2}, 10^{-4}, or 10^{-6} of the original concentration. Then 1 mℓ was transferred from the original and from each dilution to a standard, sterile tuff/water suspension. By diluting the medium and the numbers of bacteria, it was expected that a minimum and maximum effect would be observed.

The results, presented in Table IV, were not as anticipated. One would expect that with dilution there should have been a concomitant decrease in the number of bacteria, from 1.7×10^7 to 1.7×10^1 CFU. Instead, the concentration of bacteria for all dilutions was greater than 10^5 CFU. Apparently, after the 1 mℓ from each dilution was added to the tuff and water, regrowth of the bacteria occurred. This resulted in random and insignificant effects upon sorption; R_d values for the detergent experiment range from 29 to 38 mℓ/g, and values for the polymer medium vary from 34 to 47 mℓ/g. These values match those of the previous experiment for the sterile feed/nonsterile tuff, but they are much lower than those for the sterile feed/sterile tuff and bacteria.

Initially, regrowth of the microorganisms was unexpected because it was believed that the tuff/water mixture did not contain enough available

TABLE IV

PLUTONIUM SORPTION RATIOS AND BACTERIAL CONCENTRATIONS FOR A SERIAL DILUTION OF DETERGENT AND POLYMER MEDIA INOCULATED WITH BACTERIA

Sample[a]	Polymer Media		Detergent Media	
	Sorption Ratio[b] (mℓ/g)	Bacterial Concentration (CFU)	Sorption Ratio[b] (mℓ/g)	Bacterial Concentration (CFU)
Sterile feed/nonsterile tuff (nonsterile control) No media	35(1)	1.7×10^{6}	35(1)	1.7×10^{6}
Sterile feed/sterile tuff (sterile control) No media	24(1)	8.5×10^{2}	24(1)	8.5×10^{2}
Normal strength media	47(7)	8.4×10^{6}	29(1)	1.3×10^{7}
10^{-2} media dilution	37(3)	4.8×10^{5}	29(1)	4.5×10^{6}
10^{-4} media Dilution	37(5)	2.2×10^{6}	32(5)	2.7×10^{6}
10^{-6} media dilution	34(4)	4.5×10^{6}	38(5)	2.7×10^{6}

[a] Tuff GU-4-1502 (75 to 500 μm) and Well J-13 water.

[b] Numbers in parentheses represent standard deviations of the mean for duplicate samples.

substrate to support such growth. However, after reevaluation of the sterile feed/nonsterile tuff control, regrowth of microorganisms is more understandable. This control had an indigenous bacterial population of 1.71×10^6 CFU. Considering that few organic substrates are present in the tuff/water mixture, 1.71×10^6 CFU is a surprisingly high number. Apparently, bacteria are not only able to survive in a suspension of tuff and water, but also are able to grow in it. To negate the effect of bacterial growth, future sorption experiments should be conducted over a much shorter time period--perhaps as short as 2 or 3 hours.

An additional series of experiments are being conducted to determine what effect bacterial growth has on the viscosity of the detergent and polymer. Preliminary results indicate that the viscosity of both substances increases in the presence of the microorganisms. This results, in part, from biodegradation and subsequent disappearance of the surfactants. Removing the surfactants would decrease the solubility of the polymer and thereby increase the viscosity of the medium. More extensive experiments must be performed, however, before conclusions can be reached.

F. Dynamic Transport Process (R. S. Rundberg)

Pretreated groundwater samples containing a radioactive tracer (^{137}Cs, ^{133}Ba, or $^{85}Sr^{m}$) were contacted with 2-mm-thick tuff disks of 2.54-cm diameter. These tuff disks were supported by a Teflon thread immersed in the traced solution and agitated on an orbital shaker. The water was sampled periodically and analyzed to determine radionuclide uptake as a function of time. Samples were taken from as early as 5 minutes after the introduction of tracer until 4 weeks afterward.

The tuff samples, obtained from Drill Hole USW G-1 at Yucca Mountain, Nevada, were G-1-1436, a highly zeolitized ash-fall tuff from the Calico Hills; G-1-1883, a devitrified, partially welded tuff from the Prow Pass Member; and G-1-1982, a devitrified tuff also from the Prow Pass.[5,28] Radionuclides are absorbed on the zeolite minerals and smectite clays contained in the tuff matrix. The mineralogic analyses of these samples are given in Table V.

The results of these experiments were compared with the analytic solution to diffusion into a plane sheet from a solution of limited volume. This solution (equilibrium sorption and matrix diffusion) is plotted for cesium in

Fig. 4. This plot is on a log-log scale because in dimensionless form the data should be fit by simply translating the curve, that is, scaling the diffusion coefficient. It is clear that all the data cannot be fit using this model, particularly the early points.

TABLE V

X-RAY DIFFRACTION DATA

	Mineral Abundance (%)					
Tuff Sample	Smectite	Illite-Muscovite	Clino-ptilolite	Quartz	Cristo-balite	Alkali Feldspar
G-1-1436	<5	<5	75-90	5-10	---	5
G-1-1883	2-5	<5	---	20-40	0-10	40-60
G-1-1982	5-20	<5	---	---	30-60	20-60

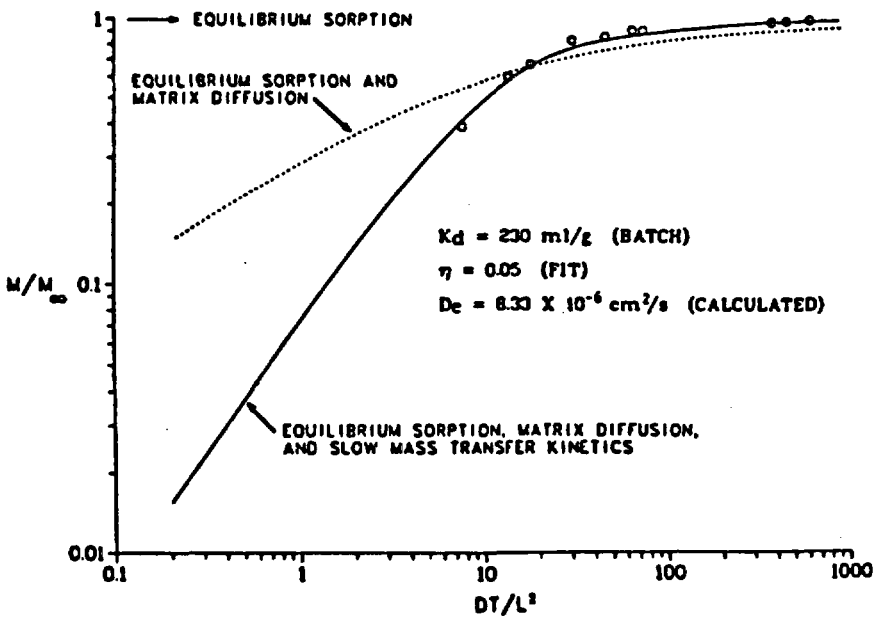

Fig. 4. Comparison of matrix diffusion with slow mass transfer kinetics and matrix diffusion with equilibration sorption (cesium).

One of the assumptions inherent in this formalism, which could affect the time dependence of uptake, is that the diffusing species is partitioned between the solid and liquid phases in a manner that is constant with time, that is, a linear adsorption isotherm. The latter assumption is valid in highly zeolitized tuff and generally in tuffs having high sorption ratios.[29] At the concentration levels used in these experiments, the isotherm is expected to be linear for the other divitrified tuffs, with the possible exception of cesium isotherms (they can be nonlinear as a result of multiple high-affinity sorption sites). Therefore, only the effect of sorption kinetics on the uptake radionuclides by tuff is discussed here.

The data were then fit to the one-dimensional diffusion equation for a plane sheet, which is coupled to a linear reversible reaction with the solid phase (defined below).

The diffusion is governed by the equation

$$\frac{\partial C}{\partial t} = D \frac{\partial^2 C}{\partial x^2} - \frac{\partial S}{\partial t} \quad ,$$

with the simultaneous reaction of the type

$$\frac{\partial S}{\partial t} = k_1 C - k_2 S \quad ,$$

where

C = concentration of the solute free to diffuse within the sheet,

S = concentration of the immobilized solute,

D = diffusion coefficient,

x = position in the disk,

t = the time, and

k_1, k_2 = the rate constants of forward and backward reactions, respectively.

The solution to these equations is given by Crank:[30]

$$\frac{M_t}{M_\infty} = 1 - \sum_{n=1}^{\infty} \frac{(1+\alpha)\exp(P_n t)}{1 + \left\{1 + \frac{k_1 k_2}{(P_n + k_2)^2}\right\}\left\{\frac{a}{2\ell} + \frac{P_n}{2Dq_n^2} + \frac{P_n^2 \ell a}{2D^2 q_n^2}\right\}} \quad ,$$

where P_n and q_n are the nonzero roots of

$$\frac{\ell P_n}{D} = q_n \tan q_n a \quad , \quad q_n^2 = -\frac{P_n}{D}\frac{P_n + k_1 + k_2}{P_n + k_2} \quad ,$$

where

$\alpha = \ell/(R + 1)a$, $M_\infty = \ell\, C_o/(1 + \alpha)$, and

C_o = the initial concentration of tracer,

a = the thickness of the sheet,

ℓ = the effective length of the solution,

M_t = the total amount of solute taken up by the sheet at time t,

M_∞ = the amount of uptake at injection time, and

$R = k_1/k_2$.

This solution is plotted in Fig. 4 as a solid line. An excellent fit to the data is obtained with diffusion coefficients that are close to what is expected for matrix diffusion. All the uptake results for the three tracers on the three tuff samples are good fits with the kinetic model. The rate constants and diffusivities are given in Table VI. Diffusion coefficients for these cations are fairly close to the free ionic diffusion coefficients. This indicates that the diffusion path is not very tortuous. However, this may not be true for the larger sample, where dead-end pores would have more effect on diffusion. In addition, although the sorption rate constants vary many orders of magnitude, the desorption rate constants vary only slightly for a given cation (less than a factor of 2 for similar tuffs and less than a factor of 4 for dissimilar tuffs).

The sorption ratios for samples of tuffs G-1-1883 and G-1-1982 were determined at 4 weeks from the distribution of radionuclides between the tuff wafer and the solution. The errors in mass balance for the G-1-1436 sample were too large to yield a meaningful sorption ratio. A desorption experiment was performed and the sorption ratios after 3 weeks were determined for cesium and strontium. The results of these experiments are shown in Table VII with corresponding measurements from crushed-tuff (batch) experiments.[11] The agreement is excellent; it differs by much less than a factor of 2 in all cases.

TABLE VI

SORPTION RATE CONSTANTS FOR NTS TUFF

Tuff Sample	Radio-nuclide	K_d (mℓ/g)	k_1 (s^{-1})	k_2 (s^{-1})	D (cm^2/s)
G-1-1436	Cs	7 790	6.3×10^{0}	1.4×10^{-4}	2.78×10^{-6}
	Sr	36 300	3.5×10^{0}	2.0×10^{-5}	2.11×10^{-6}
	Ba	148 000	1.2×10^{1}	1.7×10^{-5}	3.38×10^{-7}
G-1-1883	Cs	230	5.9×10^{-2}	4.2×10^{-5}	8.33×10^{-6}
	Sr	27	1.1×10^{-3}	6.7×10^{-6}	1.33×10^{-5}
	Ba	210	5.7×10^{-2}	4.4×10^{-5}	8.89×10^{-6}
G-1-1982	Cs	1 000	4.0×10^{-1}	4.7×10^{-5}	9.44×10^{-6}
	Sr	88	9.5×10^{-3}	1.4×10^{-5}	1.37×10^{-5}
	Ba	800	2.6×10^{-1}	4.4×10^{-5}	8.89×10^{-6}

If the rate of sorption is controlled by diffusion into zeolite and clay crystals, the rate constants k_1 and k_2 can be related to the diffusion coefficient by the equations for mass transfer in ion-exchange particles[31,32] below. The uptake of cations by a mineral is expressed

$$\frac{\partial S}{\partial t} = \frac{60\, D_{eff}}{r^2} [S_i - S]$$

$$= \frac{60\, D_{eff}}{r^2} [(\varepsilon + K_d \rho) C_m - S] \quad ,$$

so that

$$k_1 = 60\, [\varepsilon + K_d \rho] \frac{D_{eff}}{r^2} \quad , \text{ and}$$

$$k_2 = 60 \frac{D_{eff}}{r^2} \quad ,$$

where

C_m = concentration in the pore fluid,
S_i = concentration in the solid phase at the interface,
r = the crystal diameter,
D_{eff} = effective diffusion coefficient,
K_d = distribution coefficient,
ρ = dry bulk density, and
ε = porosity.

This enables one to estimate a diffusion coefficient for an ion inside the zeolite or clay crystal, assuming the film resistance on the crystal is the same for ion-exchange resin. Samples of the tuffs used in these experiments have been examined under a scanning electron microscope (SEM). The zeolite and clay crystals appear to be equal to or smaller than 1 μm in diameter. This allows one to calculate an upper limit for the intracrystalline diffusion coefficient. These estimates are reported in Table VIII, as well as diffusion coefficients determined for two pure natural zeolites (chabazite and mordenite). The diffusivities in these zeolites are many orders of magnitude smaller than the free ionic diffusivities because of the narrow channels within the zeolite crystal structure, through which the ions must

TABLE VII

K_d COMPARISON: TUFF WAFERS VS CRUSHED TUFF

Tuff Sample	Element	K_d (Wafer) (mℓ/g)	K_d (Batch) (mℓ/g)
G-1-1883 (sorption)	Sr	27	22
	Cs	230	190
	Ba	210	180
G-1-1982 (sorption)	Sr	80	62
	Cs	1 000	1 200
	Ba	800	800
G-1-1436 (desorption)	Sr	96 500	87 000
	Cs	14 900	24 000

TABLE VIII

INTRACRYSTALLINE DIFFUSION COEFFICIENTS

Sample	Ion	D (cm^2/s)
Chabazite[a]	Cs^+	4.9×10^{-13}
	Sr^{2+}	1.3×10^{-16}
	Ba^{2+}	1.3×10^{-13}
Mordenite[b]	Cs^+	5×10^{-15}
	Sr^{2+}	1.5×10^{-16}
	Ba^{2+}	4.5×10^{-16}
G-1-1436	Cs^+	$\leq 2.3 \times 10^{-14}$
	Sr^{2+}	$\leq 3.3 \times 10^{-15}$
	Ba^{2+}	$\leq 2.8 \times 10^{-14}$
G-1-1883	Cs^+	$\leq 6.7 \times 10^{-15}$
	Sr^{2+}	$\leq 1.1 \times 10^{-15}$
	Ba^{2+}	$\leq 7.3 \times 10^{-15}$
G-1-1952	Cs^+	$\leq 7.8 \times 10^{-15}$
	Sr^{2+}	$\leq 2.3 \times 10^{-15}$
	Ba^{2+}	$\leq 7.3 \times 10^{-15}$

[a] Ref. 34.

[b] Ref. 35.

migrate. The kinetic diameter of chabazite is 4.3 A and that of mordenite is 3.9 A (Ref. 33). The kinetic diameter for the zeolite clinoptilolite, which is present in the tuff of the Calico Hills of Yucca Mountain tuff G-1-1436, is 3.5 A (Ref. 33). The channel opening in a fully hydrated montmorillonite clay (the principal adsorbing mineral in G-1-1883 and G-1-1952 tuff) is approximately 5.6 A (Ref. 33). Therefore, a larger diffusivity in montmorillonite is expected. Until more complete crystal size distributions are measured in these tuffs, this difference cannot be observed. The estimated diffusivities show that the mass transfer rates observed for cesium, strontium, and barium sorption on Yucca Mountain tuff are consistent with a diffusion-limited ion-exchange mechanism.

The sorptive properties of Yucca Mountain tuff for the simple cations of strontium, cesium, and barium are consistent with a simple ion-exchange mechanism. The uptake of these radionuclides by intact samples of tuff can be described by matrix diffusion with a reversible adsorption reaction. The mass transfer kinetics is also consistent with diffusion-limited ion exchange, where the rate-determining step is diffusion into the channels within crystals of zeolites and clays. The sorption ratios for these cations on intact tuff are in excellent agreement with the sorption ratios that were determined for crushed tuff during batch technique experiments. This agreement is primarily the result of the small crystal size observed in SEM studies; that is, crushing to 100-μm grain size will not break individual crystals.

The actinides show a change in sorption ratio on the time scale of up to 12 weeks.[11] In addition, the actinides show very little or no dependence of the sorption ratio on the mineralogic composition of the tuff, in contrast to the strong dependence observed for cesium, strontium, and barium.[11] On the basis of the above interpretation of the sorption of simple cations, the actinides are (1) not sorbed through a cation-exchange mechanism, (2) present as a species that is too large to fit into the intracrystalline space in clays and zeolites, or (3) both. The apparent rates of sorption are too slow to be diffusion limited, and the sorption ratios do not correlate with minerals with high cation-exchange capacities.

G. Retardation Sensitivity Analysis (B. J. Travis)

Several topics were studied during this quarter: (1) additional calculations of heat load effects from a waste repository in Yucca Mountain, (2) a field study of plutonium and americium transport in fractured, unsaturated tuff at Los Alamos, and (3) model equations for colloid transport.

1. Heat Load Effects. In a previous report,[36] the effects of waste heat load on pore water distribution near a repository in Topopah Spring tuff were examined numerically. In particular, two computer simulations (runs 1 and 2) were performed on large-scale effects. Since run 1 and run 2 were computed, additional information has become available, and more computer calculations have been performed, two of which are briefly described here. These two additional runs (3 and 4) calculated heat flow from a single waste canister. Only one-dimensional flow perpendicular to the canister axis is considered. Heat load history was obtained from M. Revelli of the Lawrence Livermore National Laboratory. Although one calculation allows no venting, the other does.

For both later calculations, the material properties used are listed below and in Tables IX and X.

Saturated permeability (darcys)	1.0×10^{-5}
Grain density (g/cm^3)	2.5
Porosity	0.12
Saturation	0.60
Specific heat (ergs/g·°C)	0.689×10^{7}
Thermal conductivity (ergs/cm·°C·s)	1.8×10^{5}

The energy source is given in Table XI. For these preliminary one-dimensional runs, a uniform computational mesh was used, beginning with the hole radius (22 cm). Energy was deposited into the first zone of the computational mesh. For the no-venting case, no mass or energy was allowed to flow back out of the matrix into the canister hole. For the venting case, the canister hole was kept at 100 kPa pressure. Mass and energy flow from the matrix was allowed back into the canister hole if such is the tendency. The results of these calculations are summarized in Figs. 5 through 17, which are plots of normalized temperature, pressure, and saturation vs radius at selected times.

TABLE IX

MATRIC POTENTIAL VS SATURATION

Saturation	Matric Potential (bars)
0.05	500.0
0.10	100.0
0.20	60.0
0.60	10.0
0.80	1.0
0.90	0.1
0.999	0.05
1.0	0.

TABLE X

RELATIVE PERMEABILITY VS SATURATION

Saturation	Air Relative Permeability	Water Relative Permeability
0.	1.00	0.
0.018	0.96	1.8×10^{-16}
0.036	0.93	8.2×10^{-12}
0.104	0.80	8.9×10^{-9}
0.171	0.69	1.0×10^{-7}
0.233	0.58	4.7×10^{-7}
0.370	0.40	7.3×10^{-6}
0.479	0.27	5.6×10^{-5}
0.562	0.19	2.45×10^{-4}
0.617	0.15	6.6×10^{-4}
0.754	0.06	7.0×10^{-3}
0.862	0.02	0.04
0.931	0.005	0.19
0.965	0.001	0.43
1.0	0.	1.00

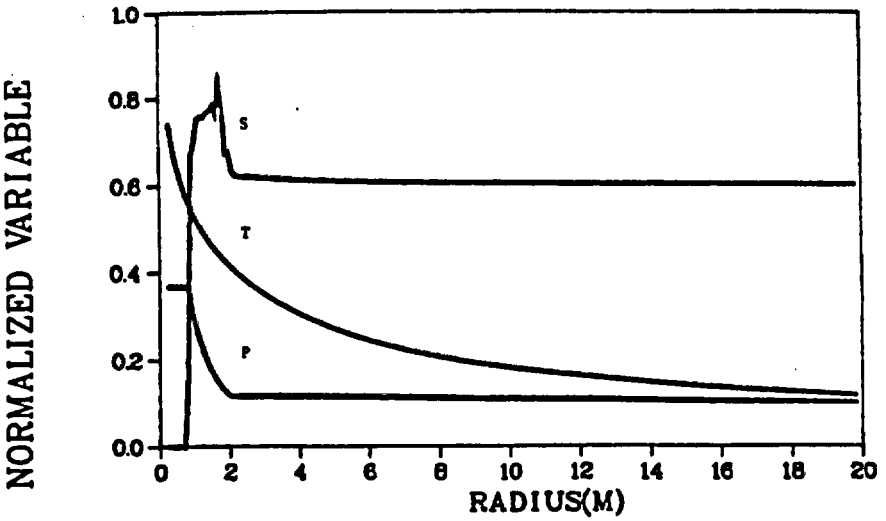

PRESSURE (KPA)	MIN=	0.	RANGE=	.100E+04
FLUID TEMP(CELSIUS)	MIN=	0.	RANGE=	.250E+03
SATURATION	MIN=	0.	RANGE=	.100E+01

Fig. 8. Saturation, temperature, and pressure profiles at 5 years for no-venting case.

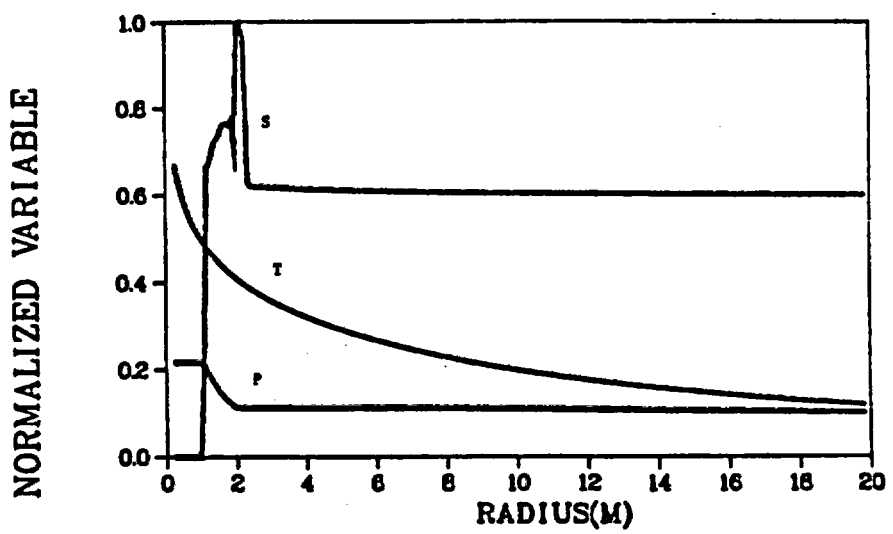

PRESSURE (KPA)	MIN=	0.	RANGE=	.100E+04
FLUID TEMP(CELSIUS)	MIN=	0.	RANGE=	.250E+03
SATURATION	MIN=	0.	RANGE=	.100E+01

Fig. 9. Saturation, temperature, and pressure profiles at 15 years for no-venting case.

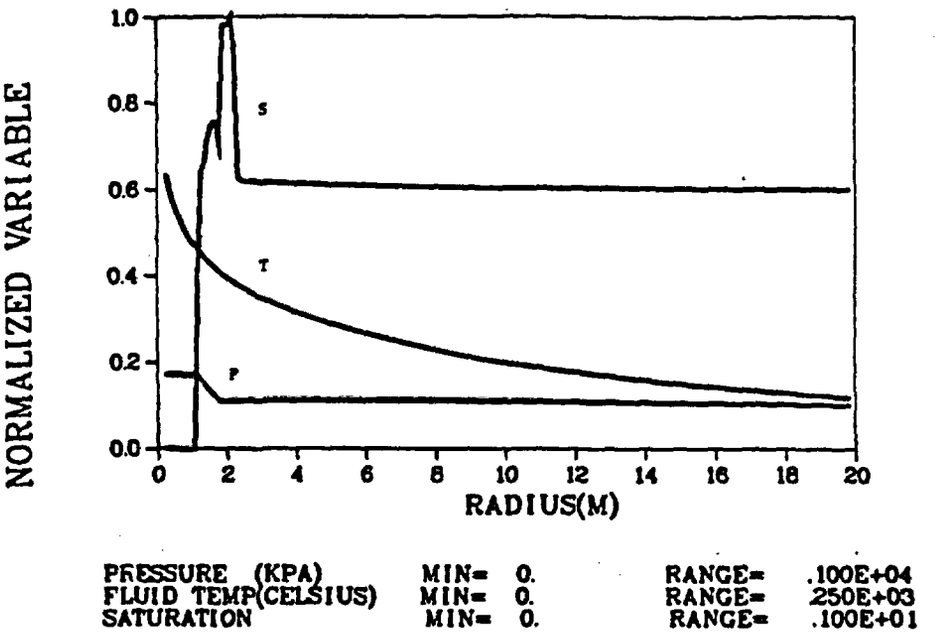

Fig. 10. Saturation, temperature, and pressure profiles at 20 years for no-venting case.

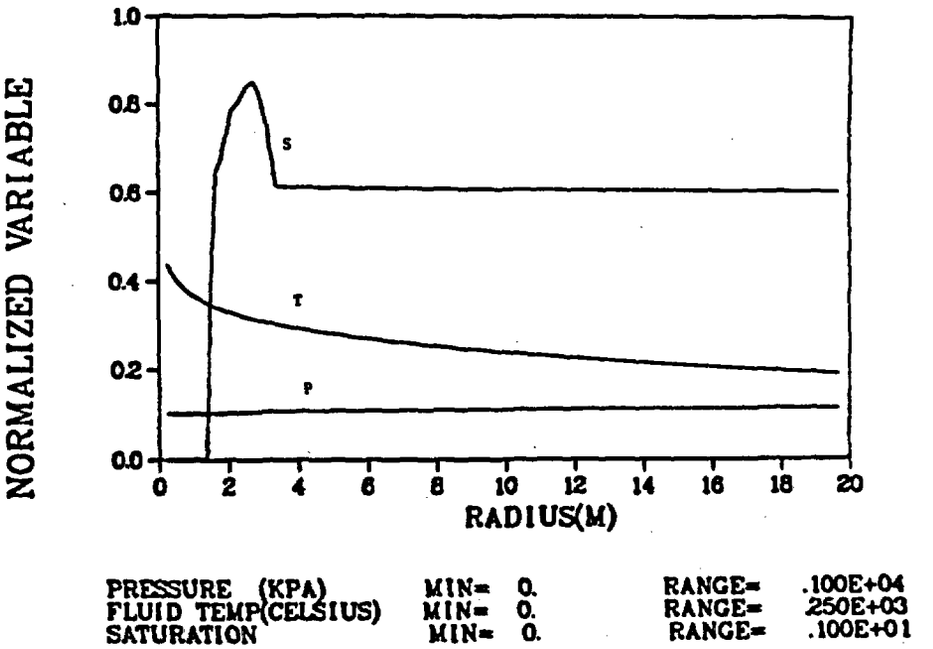

Fig. 11. Saturation, temperature, and pressure profiles at 50 years for no-venting case.

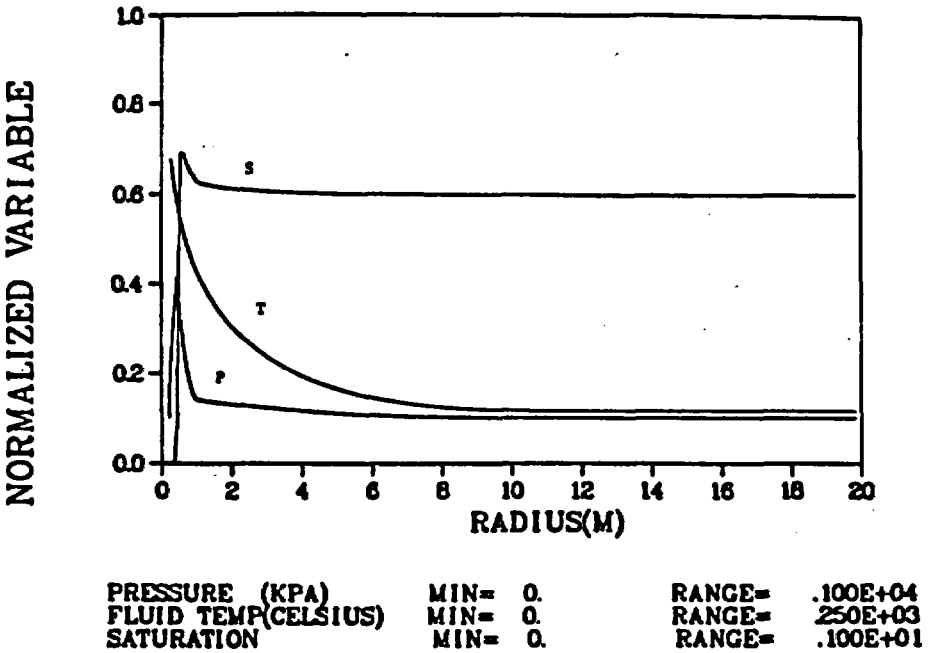

Fig. 12. Saturation, temperature, and pressure profiles at 0.5 year with venting.

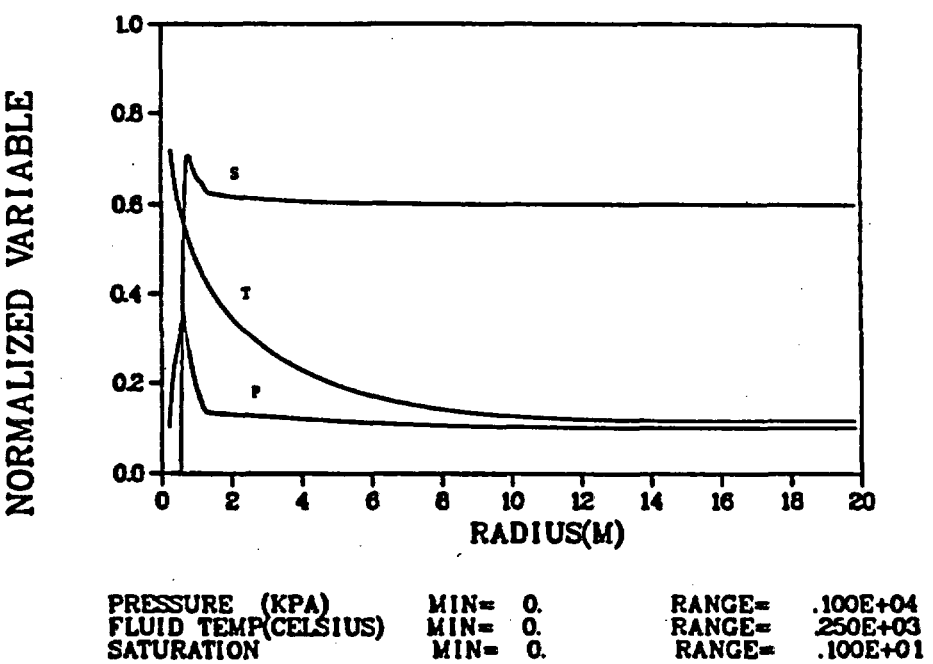

Fig. 13. Saturation, temperature, and pressure profiles at 1 year with venting.

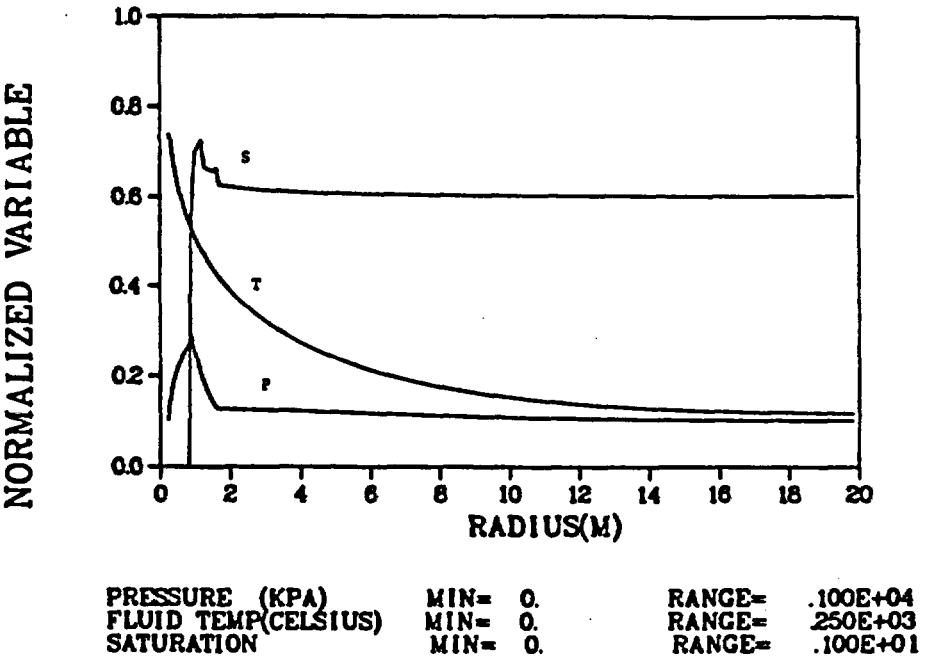

Fig. 14. Saturation, temperature, and pressure profiles at 3 years with venting.

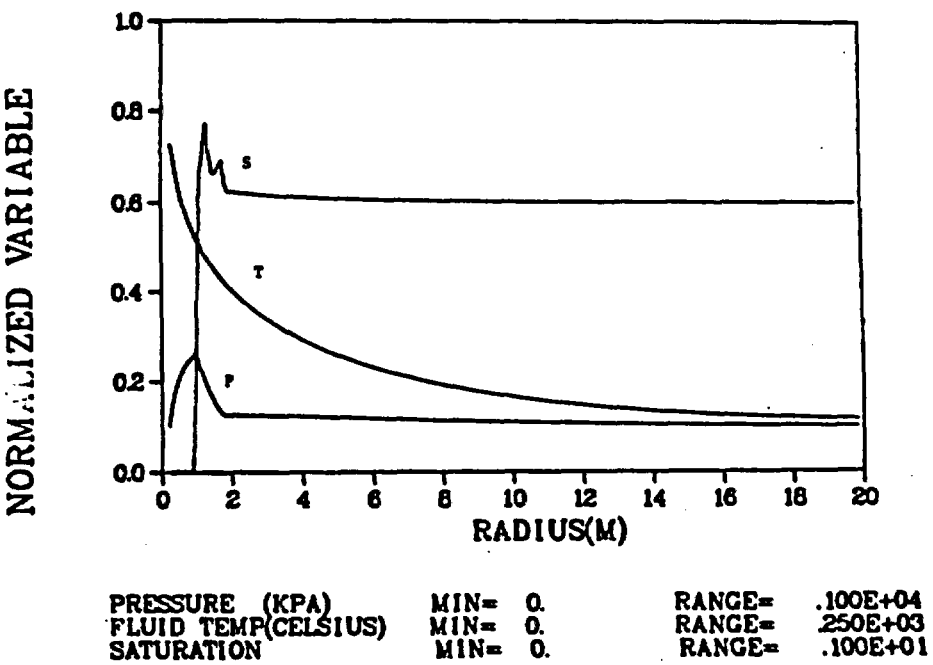

Fig. 15. Saturation, temperature, and pressure profiles at 5 years with venting.

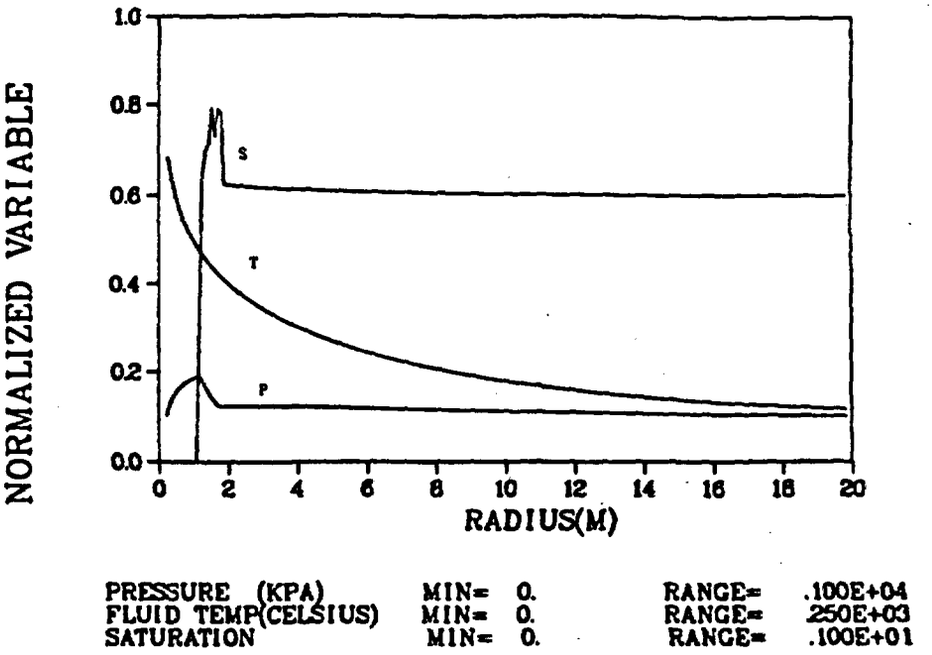

Fig. 16. Saturation, temperature, and pressure profiles at 10 years with venting.

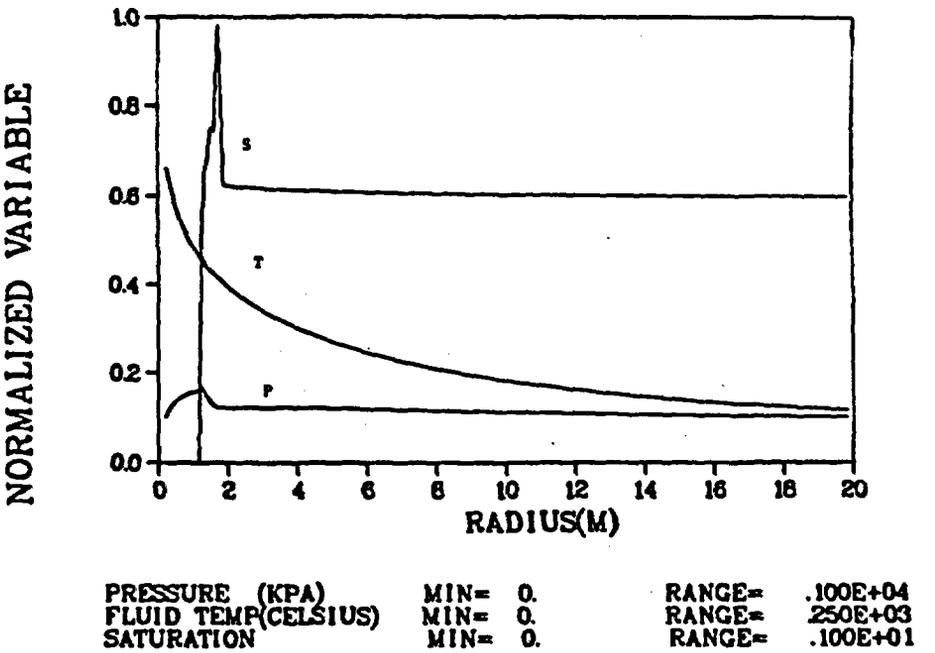

Fig. 17. Saturation, temperature, and pressure profiles at 13 years with venting.

Qualitatively, these results are the same as those found in runs 1 and 2. However, the extent of the dry-out zone (1 to 2 m) is much less because of lower matrix permeability, faster heat decay rate, and stronger matrix potential and relative permeability curves.

Venting certainly had a noticeable effect on the saturation and temperature and pressure fields. With venting, the boiling region is smaller and the saturation perturbation does not extend as far out as in the no-venting case. There is some pressure build-up in the matrix because of the low matrix permeability and vapor pressure in the boiling region.

In these calculations, as heat diffuses away from the source, water boils. The water vapor then is driven outward until it reaches cooler rock and condenses. Temperatures are buffered by the boiling process. Energy is expended in boiling water rather than raising rock temperature. Peak temperatures at the wet edge of the boiling region are only about 140°C, which is considerably lower than peak waste temperature.

2. Field Study of Radionuclide Transport in Unsaturated, Fractured Tuff. Several computer models have been developed at Los Alamos to simulate mass and heat transport in porous and fractured media. Verification (comparison to analytic solutions) of these models is a fairly easy task. Validation (comparison to experimental data) is considerably more difficult. Validation can involve laboratory data and field data. Laboratory experiments can be well controlled, but usually they do not have the length and time scales of interest. Field experiments can be closer to the desired length and time scales and also can be performed in a natural setting in or near the site of interest, but material property characterization is subject to uncertainty. The computer models have been compared successfully to a variety of laboratory experiments but to only a few semirelevant field experiments.

A set of field measurements relevant to the Yucca Mountain high-level waste storage project already exists here at Los Alamos. There are a number of studies[37] on the distribution of ^{239}Pu, ^{241}Am, and water in fractured, unsaturated Bandelier tuff beneath a former liquid-waste disposal site at Los Alamos. About 10 Ci in roughly 70 000 m^3 of liquid waste were delivered to a four-bed disposal area from 1945 to 1960. Several laboratory and field studies from 1953 to 1978 were conducted to characterize the tuff below the

disposal beds and to track the movement of plutonium and americium. In 1961, one of the beds was deliberately flooded with water in a successful attempt to change the distribution of radionuclides beneath the beds. It was found that plutonium and americium traveled at least 30 m downward and that fracture flow was ocurring. One advantage of this site is its location; additional sampling should be fairly easy.

This set of field measurements appears to be ideal for validating the computer models (such as TRACR3D) with regard to radionuclide transport in fractured, unsaturated tuff. The various reports on this field experiment are being collected and studied in preparation for computer simulations.

3. Colloid Formation and Migration Modeling. Since about 1979, the question of colloid formation and migration has increased in importance and is now a topic of major interest in the scientific community. To date, several experimental studies have shown the presence of radioactive colloids under waste disposal conditions, but their impact on repository assessment has not been addressed because the existing mathematical models that were developed to model geologic waste disposal cannot treat this problem. Additional theory and equations are required. To mathematically describe colloid formation and migration, population balance equations and submodels can be added to the existing radionuclide transport theory and codes. Through the correct use of the population balance equations and existing theory, problems of colloid formation and migration can be assessed quantitatively. The well-established theory of the population balance can also be applied to the difficult radioactive colloid problem.

During this quarter, a literature search was completed to determine the current state of colloid modeling. In addition, work has begun that will include colloid population balance model equations in the TRACR3D flow and transport code.

H. Applied Diffusion (A. E. Norris)

Field experiments have been planned to measure the rates at which solutes diffuse from solutions into the water-filled pore spaces in the proposed repository host rock and the underlying tuffaceous beds of Calico Hills. These field experiments will provide diffusivity values that can be used to calculate the rate of retardation of solute transport by diffusion

under conditions of lithostatic load and in situ saturation that would be encountered by radionuclides transported in water from the nuclear waste repository to the water table beneath Yucca Mountain. The plan for these field experiments is included in the ESTP submitted this quarter to the NNWSI waste management project manager and the technical project officers.[38]

Each diffusion experiment will be performed by the following method: (1) drill a small-diameter hole (50 mm or less) into the tuff in the main underground facility or into the tuff at the base of the ES, (2) introduce known quantities of solutes in aqueous solution into the hole, (3) seal the hole with packers for a time ranging from several months to a year, (4) overcore the tuff surrounding the drill hole, (5) transport the overcored material to Los Alamos for quantitative measurements of the solute concentration gradients, and (6) interpret the concentration gradient data as a function of the distance from the emplacement location. Diffusivities will be calculated from diffusion equations to give the best fit to the concentration gradient data.

The tracers are expected to diffuse as much as 70 mm/year from their emplacement locations, if they are not sorbed. To minimize sorption effects (and thereby maximize the distances that the tracers diffuse), the tracers to be used in this experiment will be chosen in laboratory measurements. Another problem that must be dealt with is the presence of stress relief fractures at the tracer emplacement positions. The drill holes required for this work must be about 10 m long to penetrate beyond the zone of stress relief induced by excavating the underground facilities. The small diameter of the boreholes will help minimize additional stress relief. The first experiment in each tuff will be relatively short (about 3 months) to check all phases of these diffusion experiments, including tracer analyses in the overcored tuff and data interpretation. After a successful short diffusion experiment in each tuff, a year-long experiment will be undertaken to obtain data for diffusivity values with much greater accuracy than can be obtained in a 3-month experiment.

III. MINERALOGY-PETROLOGY OF TUFF (D. Bish, D. Broxton, F. Byers, B. Carlos, R. Gooley, S. Levy, and D. Vaniman)

A. New Data on Clinoptilolite Composition

During this quarter, compilations were completed for clinoptilolite compositions in Drill Holes UE-25a#1 and b#1 and UE-25p#1. Clinoptilolite is the major sorptive zeolite at Yucca Mountain. The major variables in clinoptilolite compositions are the aluminum-to-silicon ratio and the type of exchangeable cation (magnesium, calcium, sodium, or potassium). The clinoptilolites at Yucca Mountain consist of potassium-sodium-calcium intermixed compositions; however, some calcium-rich clinoptilolites also contain small amounts of magnesium.

Four commonly zeolitized intervals at Yucca Mountain were defined in an earlier report.[9] These intervals are defined on the basis of zeolitization above the basal vitrophyre of the Topopah Spring Member (Zeolite Interval I), in the tuff of Calico Hills (Zeolite Interval II), between the Prow Pass and Bullfrog Members (Zeolite Interval III), and between the Bullfrog and Tram Members (Zeolite Interval IV). In addition to these four intervals, there are further occurrences of clinoptilolite within and below the Tram Member in some drill holes. All such occurrences can be included within Zeolite Interval V, which is discontinuous beneath Yucca Mountain.

Figure 18 shows the variations of clinoptilolite compositions in Zeolite Intervals I through IV of Drill Holes UE-25a#1 and b#1. Figure 19 shows the clinoptilolite compositions of Intervals II through V in Drill Hole UE-25p#1. The most important feature of both figures is the clustering of all compositions, from all intervals of these drill holes, in the calcium-plus-magnesium portion of the ternary projection. This lack of variation in the clinoptilolite composition between intervals is unlike that of other deep samples from Drill Holes USW G-1, G-2, GU-3, and G-3 at Yucca Mountain. In these other drill holes, clinoptilolite compositions generally become more alkali enriched (potassium plus sodium) in Zeolite Interval III, and they are finally very sodium enriched in Intervals IV and V, where the clinoptilolites may occur with analcime.[39-41]

The lack of alkali enrichment in deeper clinoptilolite intervals of Drill Holes UE-25a#1, b#1, and p#1 indicates that more than one pattern of zeolite exchangeable-cation zonation occurs at Yucca Mountain. Those holes that lack alkali enrichment at depth occur to the east of the exploration

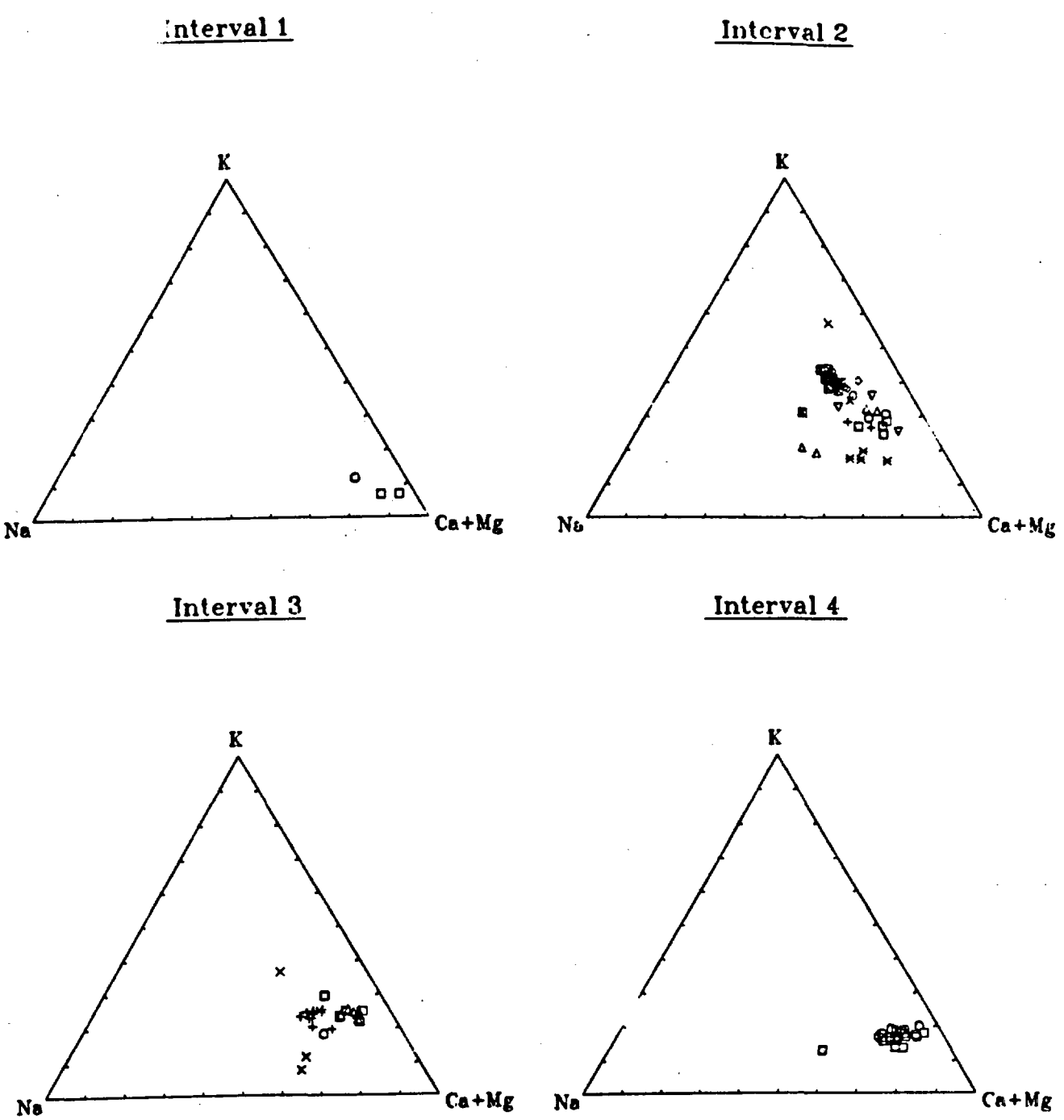

Fig. 18. Variations of clinoptilolite composition in Zeolite Intervals I through IV in Drill Holes UE-25a#1 and b#1.

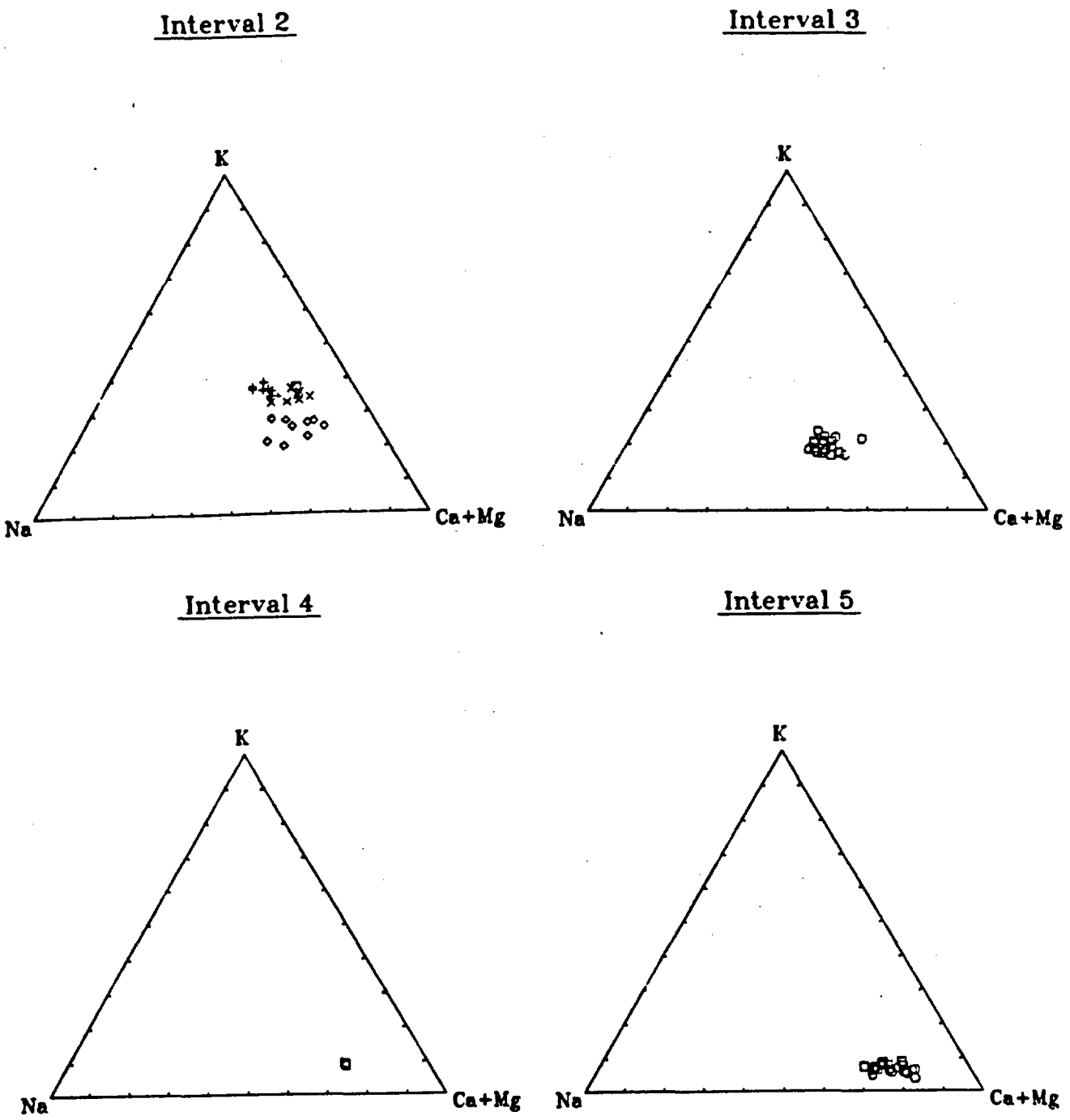

Fig. 19. Clinoptilolite composition in Intervals II through V in Drill Hole UE-25p#1.

block; data from other drill holes throughout this region are forthcoming and may help to clarify the history of zeolite development and the causes of zeolite zonation at Yucca Mountain.

B. Heating Experiments on Cristobalite, Clinoptilolite, and Heulandite.

During this quarter, high-temperature x-ray diffraction experiments were performed on cristobalite- , clinoptilolite- , and heulandite-bearing samples from Yucca Mountain drill cores. Cristobalite, which occurs in abundances of 5 to 30% in the Topopah Spring repository horizon, undergoes a volume increase upon heating. The magnitude of the increase and the temperature of transition are relevant for the heated environment in the near field. Heulandite zeolites occur in abundances up to 15% above the basal vitrophyre of the Topopah Spring Member; clinoptilolite occurs in abundances up to 75% in the zeolitized Topopah Spring base and tuff of Calico Hills. These zeolites would experience temperature rises if the waste were placed in the Topopah Spring unit, and the response of these zeolites to heating is relevant to long-term repository performance.

Stepwise heating of cristobalite-bearing samples was performed in a heating stage mounted on the Siemens D-500 diffractometer. Temperature was increased at intervals of 25°C, and $\geq$30 minutes was allowed for equilibration before x-ray diffraction analysis at each temperature. With temperature increases, the cristobalite structure changes from the α (tetragonal) to β (cubic) form through a rapid and reversible displacive transformation. Actual temperatures of transformation cited in the literature vary from 120 to 272°C (values for synthetic cristobalite vary from 257 to 271°C).[42,43] The heating experiments performed this quarter used Yucca Mountain samples from USW G-4 (1026 and 746 ft) and established for Yucca Mountain cristobalite a transformation temperature of 225 ± 25°C, with an α to β volume increase of ~5%. This temperature of transition is in close accord with the 223 ± 27°C temperature reported by Lappin[44] for samples from Yucca Mountain. These transition temperatures and those determined by other x-ray diffraction experiments (218°C, Ref. 45; 220°C, Ref. 42) contrast with those determined by calorimetric methods (257 to 271°C, Ref. 43). Because the calorimetric measurements are usually dynamic, the x-ray results are more applicable to the effects of repository-induced heating of Yucca Mountain

tuffs. For purposes of assessing the potential impact of temperature on cristobalite structure, a transformation temperature of 225 ± 25°C is applicable to a broad range of samples from Yucca Mountain.

High-temperature x-ray diffraction experiments on clinoptilolites and heulandite from Yucca Mountain were also conducted at 50°C intervals with equilibration times $\geq$30 minutes. Heulandite above the basal vitrophyre of the Topopah Spring Member (USW G-4-1314) began to invert to heulandite B at 200°C with a concomitant (reversible) volume loss of ~10%. This inversion temperature is higher than for macrocrystalline heulandite from basalts (~150°C) and probably reflects the lower aluminum content of the Yucca Mountain heulandite. The transformation proceeds more rapidly at higher temperatures, and future research will investigate the kinetics of this reaction. With heating below 200°C, heulandite from Drill Hole USW G-4 undergoes a gradual volume decrease of several per cent. Examples of x-ray diffraction patterns are shown in Fig. 20 to illustrate the changes taking place with increasing temperature. Note the significant difference in the low-angle portion of Fig. 20 between the upper pattern (300°C) and the lower pattern (100°C). Immediately below the lower Topopah vitrophyre, the zeolites are clinoptilolite rather than heulandite. Samples from Drill Hole USW G-4 at 1381 and 1392 ft do not significantly invert even at 300°C, but they undergo a minor continuous volume decrease that is typical of mixed potassium, calcium, sodium clinoptilolites. Because of the target horizon's proximity to the zeolites above the lower Topopah vitrophyre, temperatures may be high enough to transform the heulandites to heulandite B. This possibility will be addressed in future research on kinetics of the transformation.

C. Petrologic Studies of the Topopah Spring Member and Drill Hole UE-25p#1

Petrologic studies of the Topopah Spring Member in Drill Hole USW G-4 indicate that the fine, cryptocrystalline groundmass of the lower nonlithophysal (possible breakout) zone and the middle nonlithophysal zone (between the two lithophysal zones) are indistinguishable; both have a composition of high-silica rhyolite at about 77.5% SiO_2. Apparently, the middle nonlithophysal zone represents a fresh, middle ash-flow pulse after a hiatus of a few hours or a few days, during which bubbling and escape of gases from the first

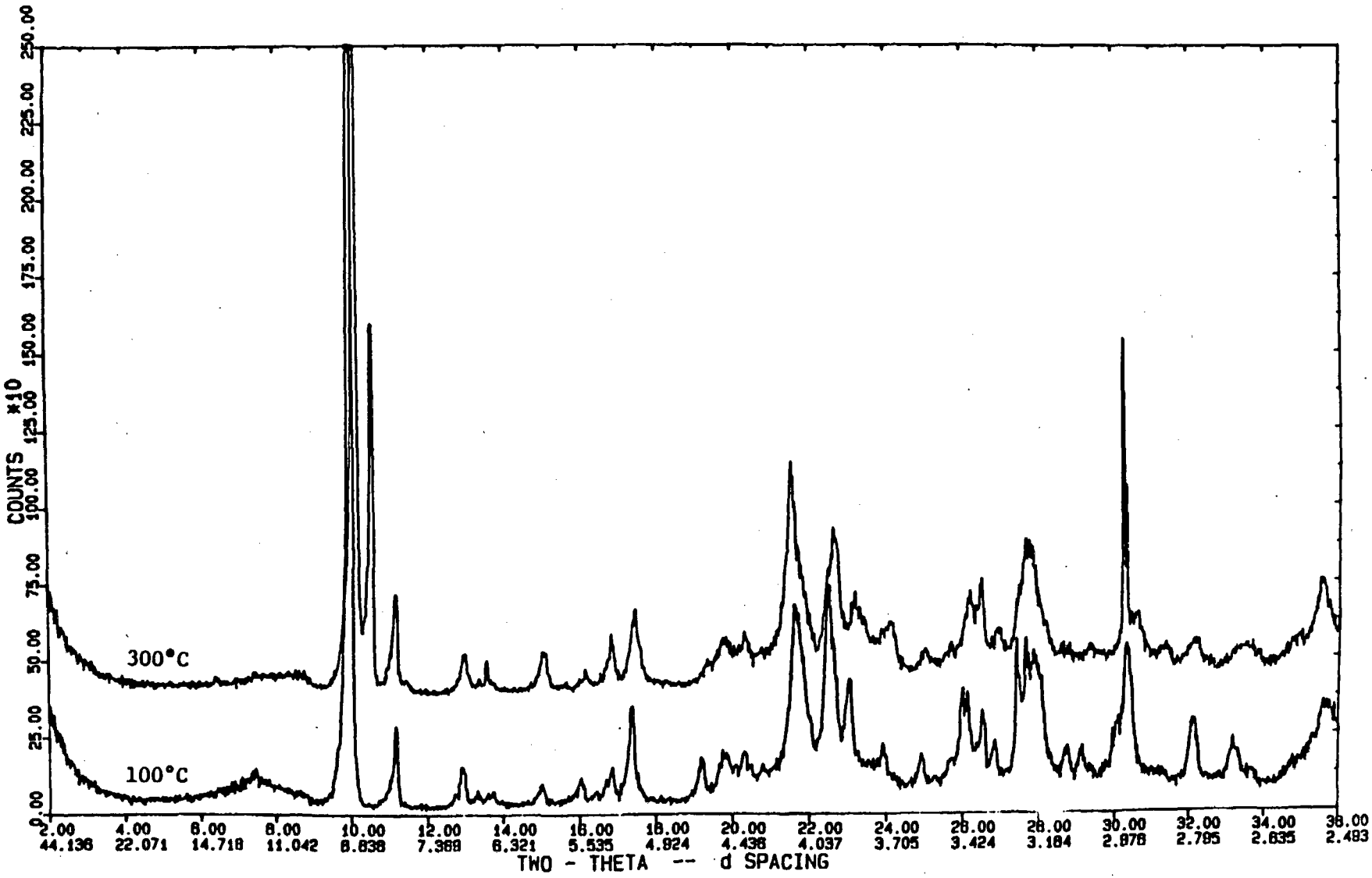

Fig. 20. Examples of x-ray diffraction patterns illustrate changes in heulandite with increasing temperature.

pulse developed the lower lithophysal zone. The lower ash flow had cooled somewhat but was still sufficiently hot and the temperature gradient was small so that chilling did not produce a medial vitrophyre. Instead, a brown cryptocrystalline zone formed, and it is almost identical to that above the basal vitrophyre. These zonal relations are also seen in Topopah Spring outcrops at Busted Butte and in other drill holes of the Yucca Mountain repository block. Evidence for such a hiatus between eruptive cycles is also cited in Carroll et al.[5] and Caporuscio et al.[39] If the basal vitrophyre or the lithophysal zones were not exposed or penetrated, it would be extremely difficult to distinguish the lower from the middle nonlithophysal zone; possibly feldspar phenocryst compositions or the greater frequency of rhyolite xenoliths in the lower nonlithophysal zone might help distinguish these subunits. Such possibilities are now being explored.

The upper crystal-rich quartz latitic petrologic zone of the Topopah Spring Member includes the partially welded uppermost zone, the thin (approximately 1-m) caprock vitrophyre, and the underlying upper vapor-phase zone. This quartz latitic composition grades downward, as lenticular flattened pumice and shards, part way into the upper part of the upper lithophysal zone, and it disappears at a depth of about 450 ft in Drill Hole USW G-4. Mixing with more silicic flow compositions is intimate down to microscopic scales. Phenocrysts of plagioclase, biotite, and clinopyroxene are commonly (but not always) enclosed in a chilled cryptocrystalline quartz latitic groundmass, which has a composition of about 72% SiO_2. These cryptocrystalline quartz latitic shards and lenticles are enclosed in a greater volume of spherulitic to granophyric (microgranular--0.05 to 0.2-mm) high-silica (77.5% SiO_2) rhyolite that is characteristic of the upper lithophysal zone.

The mineralogy and petrochemistry of the Tertiary volcanic rocks in Drill Hole UE-25p#1 has been completed, and the results were made available to the USGS for incorporation into their preliminary report. The same units that were penetrated in Drill Hole USW G-1, except the dacite flow breccia, are present in UE-25p#1. The older tuffs include two additional ash-flow tuffs below unit C; the lower of these, just above the Paleozoic contact at 4070 ft, is probably the tuff of Yucca Flat, which occurs in the lower part of Tunnel Bed 2 under Rainier Mesa and Yucca Flat.

IV. TECTONICS AND VOLCANISM (B. M. Crowe, D. T. Vaniman, D. B. Curtis, and N. W. Bower)

Volcanism studies are being conducted to evaluate the relative hazards of future volcanism with respect to storage of high-level radioactive waste. Work during the quarter concentrated on presentation of the volcanism work at the NRC Geology review meeting in Denver, a review of the NRC position paper on tectonics, refinement of the trace-element data base for basalts of the NTS region, and review of field sites for studies of hydrovolcanic deposits.

The complete volcanism program was reviewed at the NRC Geology meeting in Denver during early October. The summary talk, presented by B. Crowe, briefly described work included in published literature, work completed since printing of the report "Status of Volcanic Hazard Studies for the Nevada Nuclear Waste Storage Investigations,"[46] and remaining areas of uncertainty as listed in the current version of the SCP. These remaining areas of uncertainty include:

(1) mechanisms of emplacement of shallow basalt intrusions,
(2) origins and significance of trace-element enriched basalts of the Younger Rift Basalts,
(3) the possibility of past bimodal volcanism in the Crater Flat area,
(4) geochemical patterns of basaltic volcanism in the NTS area through time, and
(5) the possibility of future hydrovolcanic activity at the Yucca Mountain site.

Progress on topics (2), (3), and (4) was summarized in the last quarterly report.[9] No review comments were made at the NRC review meeting on the first topic, mechanisms of emplacement of shallow basalt intrusions. Work on the hydrovolcanic question is continuing during FY 1984. Another possible area of uncertainty was raised at the October meeting: whether the Death Valley-Pancake Range volcanic belt could mark an incipient zone of continental rifting. This possibility was considered several years ago during volcanic hazards studies and was considered unimportant for several reasons.

(1) The volcanic belt is expressed only in the patterns of basaltic volcanism during the last 7 Myr.
(2) There is little or no geophysical or topographic expression of the volcanic belt.

(3) The belt has existed as a distinct volcanic feature for the last 7 Myr with no increase in rates of volcanism.

To investigate the question of rift formation, it may be necessary to study seismic refraction lines shot perpendicular to the volcanic belt and of sufficient length to determine if there is any change in the geometry of the crust/mantle boundary that can be related to the belt. Ideally, this should be done across the Lunar Crater volcanic field at the north end of the belt (currently the most active part of the volcanic belt) and across the NTS area (a much less active part of the belt). This project was proposed for the volcanism studies 3 years ago but was rejected because of the cost of obtaining the geophysical data. These data may be needed if the possibility of rifting is considered an important issue.

The NRC position paper on tectonics was reviewed, and written comments on topics related to volcanism were sent to DOE. Current volcanism studies cover all aspects of the tectonic questions, with three exceptions. First, volcanic hazard assessments have concentrated on the primary effects of volcanism; secondary effects are much more broad in scope and require definition of the waste isolation system, which should be a task of performance assessment. Second, an integrated model of the tectonic setting of southern Nevada has not been developed. Volcanic patterns cannot be related to tectonic models until this work is completed. Third, questions about geothermal activity in southern Nevada are not considered significant for several reasons.

(1) There are few known thermal springs or wells in the area.

(2) Measured temperatures in the springs or wells are in the range of 22 to 42°C.

(3) Water in the springs or wells is dilute (<500 ppm), and the springs are Na-HCO_3 systems with near neutral pH (pH 7 to 9).

(4) The distribution of springs shows no relation to sites of recent volcanism.

(5) The spring distribution appears to be related to existing faults or fault systems, which suggests that the thermal waters represent upwelling of gradient-heated waters.

Trace-element data for the basalts of the NTS region have been entered into a data base management system on the VAX 11/780. The data were entered in two separate systems: (1) trace-element data obtained by an automated INAA

system and (2) more precise INAA and x-ray fluorescence analyses. Work is under way to cross-calibrate the two data analysis systems.

Field sites of known hydrovolcanic activity in the southern Great Basin were cataloged. Known sites include at least seven volcanic centers in the Lunar Crater volcanic field, the Ubehebe Craters in northern Death Valley, an unnamed site in southern Death Valley, and two centers in the Nye Canyon area.

V. TUFF LABORATORY PROPERTIES (J. D. Blacic)

During this quarter, test #TC8 was completed on tuff of Calico Hills from Drill Hole USW G-4. The history of this test is shown in Fig. 21. During the test run of 447 hours, the applied stress was varied from 32 to 40 MPa (with one unplanned excursion to 24 MPa).

The test began at 32 MPa stress and was maintained for a period of 175 hours, after which the stress dropped to 24 MPa over 2 days (beginning at point A, Fig. 21). This drop occurred inadvertently because a switch was left

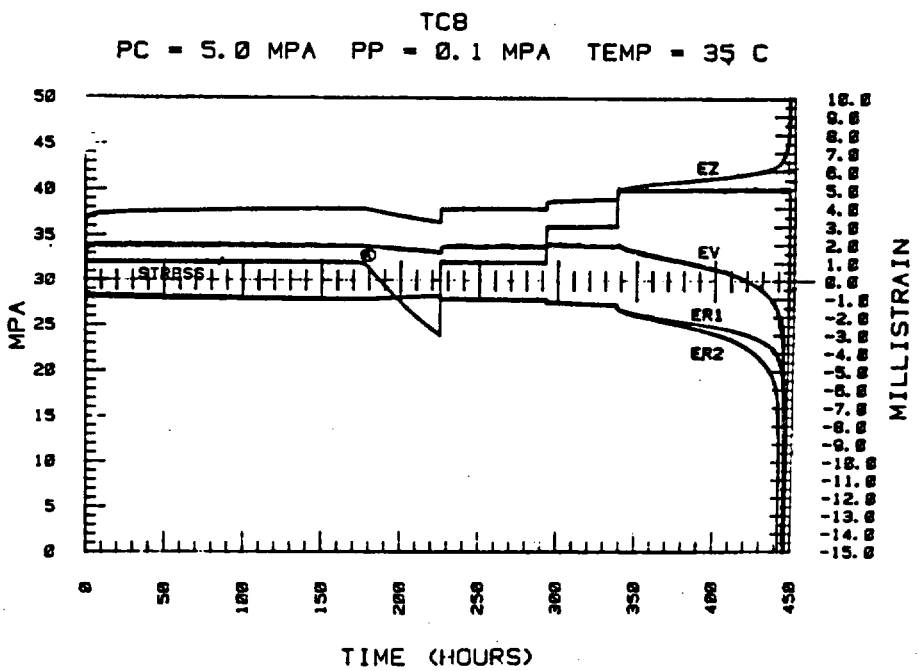

Fig. 21. History of stress test #TC8.

in the wrong position. When the error was found, the stress was raised back to 32 MPa, and the sample soon recovered to nearly the same strains and strain rates. The axial strain over this period was about 1×10^{-10} s^{-1} at 32 MPa stress. Because the strain rate was so low, the stress was increased in increments until dilatancy began. At about 292 hours, the stress was raised 4 MPa to 36 MPa. The axial strain rate increased about a factor of 5, and a slightly negative volume strain rate was produced. At about 337 hours, the stress was increased again by 4 MPa to 40 MPa. The axial strain rate increased by about another factor of 5 to $\sim 2.3 \times 10^{-9}$ s^{-1}, and a moderate rate of delatant volume strain was produced. This stress level was maintained until failure at about 447 hours. In Fig. 21, both circumferential strain gages are plotted (ER1 and ER2) to show the inhomogeneous nature and slow onset of Tertiary failure in this sample. The gages tracked one another very well until just after the last stress increase, at which time ER2 began to show increased rates of strain and eventually went off scale about 6 hours before the ultimate failure of the sample as a whole.

VI. SEALING MATERIALS EVALUATION (C. J. Duffy; D. M. Roy, Pennsylvania State University)

Concretes are being proposed as one major type of potential sealing material for a nuclear waste repository sited in the felsic tuffs of Yucca Mountain. Introduction of any sealing materials will, in general, cause reactions between the host rock and the sealant because of chemical differences and the reactive nature of fine minerals and glasses in the tuff.

Different concretes were evaluated to address the potential for chemical compatibility with the tuff rock chemistry. Two approaches to sealant/host rock compatibility were examined. The first concrete used indigenous sands and gravel in the formulation of the sealant; the second approach used more conventional concrete materials but controlled the "bulk" chemical composition of the concrete to closely match the tuff composition.

This project will evaluate the chemical stability of potential sealing materials through laboratory studies conducted under a series of conditions that represent a range of credible temperature conditions.

Different experimental designs are being used to evaluate the chemical stability of concretes that were developed to test the approach to chemical compatibility with the host tuff. Current experimental efforts are being

applied to the latter approach, in which the bulk chemical composition of the sealant is adjusted by the addition of reactive admixtures. For the purpose of this study, the admixtures are chiefly silica or silica-rich components that are added in the appropriate proportions to minimize formation of calcium hydroxide during hydration of the cementitious phases. The additions were carefully selected to provide the maximum formation of tobermorite and gyrolite, which would result in a less porous, more impermeable material.

A set of experiments that began during FY 1983 are nearly complete. These experiments included the use of (1) fine powders reacted in static conditions (cold-seal pressure vessels) at several temperatures, (2) coarser powders reacted in an apparatus designed to maximize dissolution by constantly agitating the fluids in contact with the powder, (3) monolithic disks cut from a simulated concrete, and (4) tuff prisms cast into the adjusted grout to evaluate interfacial reactions. These latter experiments are being conducted in both a static and an agitated condition and at several temperatures up to those that simulate the maximum credible repository temperature of 200°C and a much advanced temperature of 300°C. Locally derived groundwater from the Well J-13 is being used as the mineralizing fluid in all these tests.

The mortar used in these studies includes 40% of a shrinkage-compensating cement and other components and uses the formation of the mineral ettringite to prevent shrinkage. Physical properties measurements on this formulation, carried out on the Sandia project, suggested further investigation of this material's stability. The compressive strength of the mortar is high, generally about 100 MPa after early curing up to about 1 week, and testing at 6 months has produced compressive strengths of about 160 MPa. Water permeability measured on the mortar and mortar/tuff composite samples is typically very low. The permeability of the composite samples is always limited by the permeability of the tuff to the range of microdarcies. The mortars are typically at the limits of our instrumentation for measurements of a few days duration: 10 ndarcy.

Solutions in contact with the granular concrete solids and the disk samples were recovered "at temperature" and, in some cases (depending upon the experimental design), at room temperature. Because the last set of samples has just been finished, a complete data set for the disk experiments is not yet available. The fluid analyses of the rocking autoclave samples,

however, is now complete. The pH of the fluids recovered at temperature and pressure from the rocking autoclave, after subsequent cooling to room temperature, was initially recorded at 8.8 at 1 hour; gradually, over the 1000 hours of the experiment, it decreased to about 6.8. A comparison of the final at-temperature value and the room temperature value obtained at the termination of the experiment showed a slight increase to 6.95: a value in the nominal range of the observed Well J-13 waters.

Chemical analyses for 17 elements in the fluids recovered on a sampling interval approximating 2^n hours show that calcium, potassium, sodium, and silica are the dominant cations and NO_3^- and SO_4^{2-} are the dominant anions. The total dissolved solids for the major oxides are about doubled in concentration in the hydrothermal fluids compared to the totals in Well J-13 water (see Table XII). Calcium, potassium, and NO_3^- have approximately the same concentrations, whereas silica and sulfate are enriched fourfold and sevenfold, respectively, in the hydrothermal fluid (Table XII). Magnesium exhibits a 75% reduction in the concentration, and sodium shows a 25% reduction in the hydrothermal fluids, compared to the Well J-13 water.

Time vs concentration plots for these data sets suggest that at about 400 hours into the experiment a steady state of alteration has been reached with very little change in concentration occurring over the next 600 hours of the test. A direct correlation in the solubility behavior between calcium and sufate is present in the data sets. This behavior can be attributed to the presence of anhydrite at temperature and gypsum in the room temperature sample. The solubility recorded in the fluids is at about 0.5 the saturation value for anhydrite reported by Blount and Dickson[47] and about 7% of the gypsum value. The sulfate-to-calcium ratio at temperature is 6:1 and at room temperature is 3:1. The presence of sulfate in the leachate is directly attributable to the decomposition of the phase responsible for the expansive properties of the concrete ettringite.

In addition, the leachate is enriched in silica relative to the Well J-13 groundwater. The recorded value is slightly supersaturated with respect to quartz at 200°C, the nominal operating temperature of the experiment, but it is less than that of amorphous silica.

An SEM/EDX characterization of the reaction product solid phase provided complementary information for the disk studies. The bulk qualitative

TABLE XII

CONCENTRATIONS OF WELL J-13 GROUNDWATER AND FLUID IN CONTACT WITH 82-22 AFTER HYDROTHERMAL TREATMENT

	Well J-13 Water (millimole/ℓ)	82-22 Fluid (millimole/ℓ)
CaO	0.29	0.30
MgO	0.07	0.02
K_2O	0.13	0.16
Na_2O	1.96	1.45
SiO_2	0.53	2.08
SO_4^{2-}	0.19	1.30
NO_3^-	0.16	0.21

chemistry and the morphologies of the reaction products are similar to those observed in the disk experiments.

VII. EXPLORATORY SHAFT

A. Technical Direction - Design (D. C. Nelson and D. A. York)

WX-4 and WX-6 personnel reviewed two draft versions of the ESTP during the report period. They attended two ESTP Committee meetings (October 20-21 and November 17-18, 1983) to discuss the drafts. Estimated costs and schedules were prepared by the ESTP committee members for each of the 25 proposed ES tests. Group WX-4 summarized the estimated costs and schedules in Chap. 8 of the ESTP.

A meeting was held November 10, 1983, with K. Beall, Sandia National Laboratories, to discuss the ES design and the integration of the ES with the repository design.

S. D. Francis witnessed a successful drop test of the ES cage at Lake Shore, Inc., Iron Mountain, Michigan, on November 22-23, 1983. The headframe has been delivered to the NTS.

In anticipation that the three-level QA program that was proposed by the Los Alamos QA organization will be approved, the ES design and construction effort was broken down into its activities, components, and systems. The QA levels are being assigned for each of these items. After agreement is reached on the individual QA levels, the NQA-1 criteria will be determined for each.

B. Test Plan (C. W. Myers and J. C. Rowley)

A major milestone was achieved by the ESTP Committee this quarter: the working draft of NVO-244 "Test Plans for Exploratory Shaft at Yucca Mountain" (Ref. 33) was submitted on November 28, 1983 to NVO-WMPO and NNWSI TPOs for review. Almost all work by the ESTP committee during the quarter was directed toward completion of the draft ESTP. This work included completion of early draft versions of the ESTP for review and revision at committee meetings held October 20-21, 1983, and November 17-18, 1983, at the SAI office in Las Vegas. Details of this work are in the October and November monthly reports.

The draft ESTP is organized into two parts. The first part contains chapters on the geologic setting, rationale for tests, shaft and drift construction operations, integrated data system, cost and schedule estimates, management, QA, safety, and environmental effects. The rationale chapter attempts to link

(1) 10CFR60 (Ref. 16) to NNWSI issues,

(2) NNWSI issues to site-specific parameters and conditions that must be assessed through ES testing, and

(3) parameters and conditions to specific tests.

The rationale chapter is a key component and needs further work. The ESTP committee will give special attention to the rationale chapter next quarter. The second part of the ESTP is a detailed description of each individual test.

C. W. Myers and D. Nelson attended the DOE/NRC pre-SCP (Site Characterization Plan) meetings on HLW repository design, exploratory shaft, and in-situ testing for the salt program in Columbus, Ohio, on October 25-26, 1983, and (with J. Fiore, DOE-NV) for the basalt program in Richland, Washington, on November 29 to December 1, 1983. Valuable insights were gained regarding the need for modifications to the rationale portions of the

NNWSI ESTP. In addition, a review of an early draft of the ESTP was completed by Golden Associates. This review will be studied by the committee and used in future work on the ESTP, especially the rationale chapter.

The following tentative schedule for future work on the ESTP is currently in effect.

February 1, 1984	TPOs forward review comments to C.W. Myers
March 28-30, 1984	WMPO/TPO/ESTP Committee "retreat" for in-depth review and discussion of ESTP
May or June 1984	Peer Review of ESTP
July or August 1984	NRC Workshop on ESTP
September or October 1984	Delivery of ESTP to Headquarters

C. Integrated Data System (D. Croy)

Work this quarter focused on completion of the IDS portion of the ESTP and on procurement actions for the IDS development system.

Writing the IDS portion of the ESTP (Part I, Chap. 9) involved analysis of all principal investigators' (PI) test plans and iterative redesign of the IDS to ensure that it would satisfy the changing requirements of the PIs. In many cases, suggestions were provided to the PIs to improve their data acquisition planning or to improve the text of the test plans. The resultant test plan provides an IDS that meets the needs expressed in the overall plans for all tests.

Procurement actions were submitted for all of the major components of the IDS development system. It is particularly important that these initial actions be done correctly. The justification packages are structured to cover the anticipated needs of the entire project. Approval of this year's procurements will allow us to purchase the same type of equipment for the Nevada installation without repeating the justification and/or vendor competition process, which will save a great deal of time and effort in the next few years. In addition, where QA is required (preaward surveys, incoming inspection, etc.), this year's actions will reduce work and schedule risks in coming years. (For example, this quarter Hewlett Packard qualified as a supplier of computers, software, and data acquisition equipment for NNWSI.)

In conjunction with the above activities, the conceptual design for the IDS has been essentially completed. The report on this conceptual design is due in February.

VIII. QUALITY ASSURANCE (R. R. Geoffrion)

A. Los Alamos

Revision 4 of the Los Alamos NNWSI Quality Assurance Program Plan was distributed for review and approval. Also in the final approval process are one new QA detailed procedure, three revised QA detailed procedures, a work plan, and a revised technical detailed procedure. Three technical detailed procedures were prepared.

The QA staff reviewed and commented on the proposed NQA-1 research and development related supplements and appendexes.

Two QA training sessions were held for Los Alamos NNWSI personnel. A milestone chart for QA activities through calendar year 1991 was prepared.

All INC-11 measuring and test equipment was reviewed for proper calibration status.

The QA sections for the draft geological sample curation facility proposal were prepared.

The Exploratory Shaft Quality Assurance Program Plan was reviewed and revised. A presentation on ES QA levels approach was made to D. Vieth. The Holmes and Narver NNWSI Records Management Study was reviewed and comments were transmitted to the WPMO. The F&S hoist wire rope specification was reviewed and comments were given to the preparer. A QA preaward survey was performed at Hewlett-Packard in Cupertino, California, for the ES IDS contract.

B. USGS

Twelve technical procedures were reviewed and submitted for approval signatures, and the tectonic studies detailed procedure was reviewed.

A 6-month surveillance schedule was developed to review all USGS NNWSI activities, and the detailed QA procedure for surveillance was circulated for approvals. Surveillance activities were performed at the instrument installation and the stemming operations at the Drill Hole UZ-1.

The QA staff represented the USGS at the DOE/NVO Audit on October 12 and 13, 1983.

ACKNOWLEDGMENTS

The following Los Alamos National Laboratory personnel are acknowledged for their efforts: D. A. Mann (technical assistance); P. A. Elder, M. E. Lark, and S. Lermuseaux (sample counting and gamma-spectra analyses); and L. M. Mitchell (typing of drafts and final manuscript).

REFERENCES

1. J. R. Smyth, "Zeolite Stability Constraints on Radioactive Waste Isolation in Zeolite-Bearing Volcanic Rocks," J. Geology 90, 195-201 (1982).

2. W. R. Daniels, B. R. Erdal, and D. T. Vaniman, Comps., "Research and Development Related to the Nevada Nuclear Waste Storage Investigations, July 1--September 30, 1982," Los Alamos National Laboratory report LA-9577-PR (March 1983).

3. D. B. Hawkins, R. A. Sheppard, and A. J. Gude, 3rd, "Hydrothermal Synthesis of Clinoptilolite and Comments on the Assemblage Phillipsite-Clinoptilolite-Mordenite" in Natural Zeolites: Occurrence, Properties, Use, L. B. Sand and F. A. Mumpton, Eds. (Pergamon Press, 1978).

4. F. Caporuscio et al., "Petrologic Studies of Drill Cores USW-G2 and UE25b-1H, Yucca Mountain, Nevada," Los Alamos National Laboratory report LA-9255-MS (July 1982).

5. D. L. Bish, F. A. Caporuscio, J. F. Copp, B. M. Crowe, J. D. Purson, J. R. Smyth, and R. G. Warren, "Preliminary Stratigraphic and Petrologic Characterization of Core Samples from USW-G1, Yucca Mountain, Nevada," Los Alamos National Laboratory report LA-8840-MS (November 1981).

6. D. B. Hawkins, "Kinetics of Glass Dissolution and Zeolite Formation under Hydrothermal Conditions," Clays Clay Miner. 29, 331-340 (1981).

7. Cheng-Hang Chi and L. B. Sand, "Synthesis of Na- and K-Clinoptilolite End Members," Nature 255-257 (1983).

8. J. D. Rimstidt and H. L. Barnes, " The Kinetics of Silica-Water Reactions," Geochim. Cosmochim. Acta 44, 1683-1699 (1980).

9. E. A. Bryant and D. T. Vaniman, Comps., "Research and Development Related to the Nevada Nuclear Waste Storage Investigations, July 1--September 30, 1983," Los Alamos National Laboratory report LA-10006-PR (July 1984).

10. R. J. Silva, "The Behavior of Americium in Aqueous Carbonate Systems," in Proceedings of the Seventh International Symposium on the Scientific Basis for Nuclear Waste Management, Materials Research Society 1983 Annual Meeting, Boston, Massachusetts, November 14-17, 1983 (to be published).

11. W. R. Daniels, K. Wolfsberg, R. S. Rundberg, A. E. Ogard, J. F. Kerrisk, C. J. Duffy, et al., "Summary Report on the Geochemistry of Yucca Mountain and Environs," Los Alamos National Laboratory report LA-9328-MS (December 1982).

12. T. W. Newton and V. L. Rundberg, "The Pu(IV) Polymer: Its Formation and Chemistry in Dilute Aqueous Solutions," in Proceedings of the Seventh International Symposium on the Scientific Basis for Nuclear Waste Management, Materials Research Society 1983 Annual Meeting, Boston, Massachusetts, November 14-17, 1983 (to be published).

13. C. Madic, G. M. Begun, D. E. Hobart, and R. L. Hahn, "Raman Spectroscopy of Neptunyl and Plutonyl Ions in Aqueous Solution: Hydrolysis of Np(VI) and Pu(IV), and Disproportionation of Pu(V)," submitted to Inorganic Chemistry.

14. D. Rai and D. A. Moore, "Solubility Product of Pu(IV) Hydrous Oxide and Equilibirum Constants of Pu(IV)/Pu(V), Pu(IV)/Pu(VI) and Pu(V)/Pu(VI) Couples," submitted to Radiochim. Acta.

15. D. A. Costanzo, R. E. Biggers, and J. T. Bell, "Plutonium Polymerization. I. A Spectrophotometric Study of the Polymerization of Plutonium (IV)," J. Inorg. Nucl. Chem., 35, 609 (1973).

16. Code of Federal Regulations, Title 10-Energy. Chap. I-NRC, Part 50: Domestic Licensing of Production and Utilization Facilities, App. B (January 1, 1982 rev.) [10-CFR-60].

17. A. P. Smirnov Averin, G. S. Kovalenko, N. P. Ermoloev, and N. N. Krot, "Microvolumetric Complexometric Determination of Np with EDTA," Anal. Chem. (USSR) 21, 62 (1966).

18. D. Rai and J. L. Ryan, "Crystallinity and Solubility of Pu(IV) Oxide and Hydrous Oxide in Aged Aqueous Suspensions," Radiochim. Acta 30, 213 (1982).

19. D. Rai and J. L. Swanson, "Properties of Plutonium(IV) Polymer of Environmental Importance," Nucl. Technol. 54, 107 (1981).

20. D. Cohen, "Electrochemical Studies of Plutonium Ions in Perchloric Acid Solution," J. Inorg. Nucl. Chem. 18, 207 (1961).

21. W. D. Schults, "Applications of Controlled-Potential Coulometry to the Determination of Plutonium," Talanta 10, 833 (1963).

22. D. Cohen and J. C. Hindman, "Oxidation Potentials of Neptunium(III)-(IV) in Perchloric Acid," J. Am. Chem. Soc. 74, 4679 (1952).

23. R. W. Stromatt, "Analysis for Neptunium by Controlled Potential Coulometry," General Electric Company, Richland, Washington, report HW-59447 (1959).

24. D. Cohen, "The Absorption Spectra of Plutonium Ions in Perchloric Acid Solutions," J. Inorg. Nucl. Chem. 18, 211 (1961).

25. K. Wolfsberg, D. T. Vaniman, and A. E. Ogard, Comps., "Research and Development Related to the Nevada Nuclear Waste Storage Investigations, January 1--March 31, 1983," Los Alamos National Laboratory report LA-9793-PR (June 1983).

26. A. E. Ogard, K. Wolfsberg, and D. T. Vaniman, Comps., "Research and Development Related to the Nevada Nuclear Waste Storage Investigations, April 1--June 30, 1983," Los Alamos National Laboratory report LA-9846-PR (December 1983).

27. "Procedures for Collecting Soil Samples and Methods of Analysis for Soil Survey," Soil Survey Investigation No. 1 (US Department of Agriculture, Soil Conservation Service, Washington, DC, August 1982 rev.)

28. R. W. Spengler, F. M. Byers, Jr., and J. B. Warner, "Stratigraphy and Structure of Volcanic Rocks in USW-G1, Yucca Mountain, Nye County, Nevada," US Geological Survey open-file report 81-1349 (1981).

29. K. Wolfsberg, R. D. Aguilar, B. P. Bayhurst, W. R. Daniels, S. J. DeVilliers, B. R. Erdal, F. O. Lawrence, S. Maestas, A. J. Mitchell, P. Q. Oliver, N. A. Raybold, R. S. Rundberg, J. L. Thompson, and E. N. Vine, "Sorption-Desorption Studies on Tuff. III. A Continuation of Studies with Samples from Jackass Flats and Yucca Mountain, Nevada," Los Alamos National Laboratory report LA-8747-MS (May 1981).

30. J. Crank, The Mathematics of Diffusion, 2nd ed. (Oxford University Press, London, 1975), p. 135.

31. T. K. Sherwood, R. L. Pigford, and C. R. Wilke, Mass Transfer, (McGraw-Hill, New York, 1975), p. 580.

32. T. Vermeulen, G. Klein, and N. K. Hiester, Chemical Engineers' Handbook, J. H. Perry, Ed. (McGraw-Hill, New York, 1973), Sec. 16.

33. D. W. Breck, Zeolite Molecular Sieves (John Wiley & Sons, New York, 1974).

34. R. M. Barrer, R. Bartholomew, and L. V. C. Rees, "Ion Exchange in Porous Crystals. I. Self- and Exchange-Diffusion of Ions in Chabazite," J. Phys. Chem. Solids 24, 51-62 (1963).

35. A. V. Rao and L. V. C. Rees, "Kinetics of Ion Exchange in Mordenite," Trans. Faraday Soc. 62, 2505 (1966).

36. B. J. Travis, S. W. Hodson, H. E. Nuttall, T. L. Cook, and R. S. Rundberg, "Numerical Simulation of Flow and Transport in Partially Saturated, Fractured Tuff," in Proceedings of the Seventh International Symposium on the Scientific Basis for Nuclear Waste Management, Materials Research Society 1983 Annual Meeting, Boston, Massachusetts, November 14-17, 1983 (to be published).

37. J. W. Nyhan, B. J. Drennan, M. L. Wheeler, W. D. Purtyman, G. Trujillo, J. Herrera, and J. W. Booth, "Environmental Migration of Long-Lived Radionuclides Beneath a Former Los Alamos Liquid Waste Disposal Site After 33 Years," Los Alamos National Laboratory document LA-UR-83-1199.

38. "Test Plans for the Exploratory Shaft at Yucca Mountain," US Department of Energy, Nevada Operations Office report NVO-244, Rev. 0 (November 28, 1983).

39. F. Caporuscio, D. Vaniman, D. Bish, D. Broxton, B. Arney, G. Heiken, F. Byers, R. Gooley, and E. Semarge, "Petrologic Studies of Drill Cores USW G-2 and UE25b-1H, Yucca Mountain, Nevada," Los Alamos National Laboratory report LA-9255-MS (July 1982).

40. F. Caporuscio, R. Warren, and D. Broxton, "Detailed Petrographic Descriptions and Microprobe Data for Tertiary Silicic Rocks in Drill Hole USW G-1, Yucca Mountain, Nevada," Los Alamos National Laboratory report LA-9323-MS (to be published).

41. D. Vaniman, D. Bish, D. Broxton, F. Byers, G. Heiken, B. Carlos, E. Semarge, F. Caporuscio, and R. Gooley, "Variations in Authigenic Mineralogy and Sorptive Zeolite Abundance at Yucca Mountain, Nevada, Based on Studies of Drill Cores USW GU-3 and USW G-3," Los Alamos National Laboratory report LA-9707-MS (June 1984).

42. D. R. Peacor, "High-Temperature Single-Crystal Study of the Cristobalite Inversion," Zeit. Kristallog. 138, 274-298 (1973).

43. P. Richet, Y. Bottinga, L. Denielou, J. P. Petitet, and C. Tequi, "Thermodynamic Properties of Quartz, Cristobalite and Amorphous SiO_2: Drop Calorimetry Measurements Between 1000 and 1800 K and a Review from 0 to 2000 K," Geochim. Cosmochim. Acta 46, 2639-2658 (1983).

44. A. R. Lappin, R. G. Van Buskirk, D. O. Enniss, S. W. Butlers, F. M. Prater, C. S. Muller, and J. L. Bergosh, "Thermal Conductivity, Bulk Properties, and Thermal Stratigraphy of Silicic Tuffs from the Upper Portion of Hole USW-G1, Yucca Mountain, Nye County, Nevada," Sandia National Laboratories report SAND81-1873 (1982).

45. W. Johnson and K. W. Andrews, "An X-ray Study of the Inversion and Thermal Expansion of Cristobalite," Br. Ceramic Soc. Trans. 55, 227-235 (1956).

46. B. M. Crowe, D. T. Vaniman, and W. J. Carr, "Status of Volcanic Hazard Studies for the Nevada Nuclear Waste Storage Investigations," Los Alamos National Laboratory report LA-9325-MS (March 1983).

47. C. W. Blount and F. W. Dickson, "Gypsum-Anhydrite Equilibria in Systems $CaSO_4$-H_2O and $CaCO_4$-NaCl-H_2O," Am. Min. 58, 323-332 (1973).

•U.S. GOVERNMENT PRINTING OFFICE: 1984-0-776-026/4169